Pleistocene Coral Reef Terraces on the Saudi Arabian Side of the Gulf of Aqaba, Red Sea

Marco Taviani, Paolo Montagna, Najeeb M. A. Rasul, Lorenzo Angeletti, and William Bosworth

Abstract

A major geomorphic feature of the coastal Red Sea region is represented by Pleistocene raised marine terraces that occur on both sides of the Gulf of Aqaba. Those bordering the Saudi Arabian sector have received little attention thus far, and are comparatively less known than their counterparts in the Sinai sector of the Gulf and in the Red Sea. As is the rule in the Red Sea region, the best developed marine terrace system is reefal and pertains to the last interglacial (Marine Isotope Stage 5e = MIS5e, ~125 ka BP), although older Pleistocene terraces also occur. All such deposits are very fossiliferous and most carbonates are relatively unaltered, providing suitable material for geochronological purposes. Syndepositional marine botryoidal aragonite cements have been identified infilling vugs in the host bedrock at some sites. In some respect, the MIS5e deposits are unique, reflecting the structurally-controlled bedrock geology and the Gulf's topography. The Gulf of Aqaba is rather narrow and characterized by steep and precipitous topography along its flanks. Coastal marine deposits commonly plaster the crystalline Arabian basement which faces the present seashore, extending from the Jordan border to almost two thirds of the coastal strip. Terraces sitting on this basement have been tectonically uplifted to considerable altitudes (up to 26 m) over the present mean sea level (m.s.l.). The bulk of the marine deposits represent upper fore-reef to beach settings, with better developed back-reef to lagoonal facies only preserved in those favourable conditions (wadi valleys) where sufficient accommodation space was available during the MIS5e to allow inland marine expansion. This is observed in the north at Al Wasel, and ~14 km south of Ra's Suwayhil as Saghir. The terraces further to the south lie instead over a more recent bedrock, including Miocene sedimentary strata. Here MIS5e deposits are found close to standard altitudes between ~4–8 m above present m.s.l., and preserve shallow reefal habitats, as seen at Ash Shaykh Humayd. A rare example of a putative MIS5e salina-mangal complex has been identified in the area of Ra's Suwayhil as Saghir at ~23 m above m.s.l.

M. Taviani · P. Montagna · L. Angeletti (✉)
Istituto di Scienze Marine (ISMAR-CNR), Via Gobetti 101, 40129 Bologna, Italy
e-mail: lorenzo.angeletti@bo.ismar.cnr.it

M. Taviani
e-mail: marco.taviani@bo.ismar.cnr.it

M. Taviani
Biology Department, Woods Hole Oceanographic Institution, 266 Woods Hole Road, Woods Hole, MA 02543, USA

M. Taviani
Stazione Zoologica Anton Dohrn, Villa Comunale, 80121 Naples, Italy

P. Montagna
Lamont-Doherty Earth Observatory, Columbia University, 61 Route 9W, Palisades, NY 10964, USA

N. M. A. Rasul
Center for Marine Geology, Saudi Geological Survey, Jeddah, Saudi Arabia

W. Bosworth
Apache Egypt Companies, 11 Street 281, New Maadi, Cairo, Egypt

1 Introduction

Raised terraces representing prevalent former coral reef systems stretch discontinuously the entire length of the Red Sea, including islands, and the Gulf Aden (e.g., Hume and Little 1928; Dreyfuss 1931; Sandford and Arkell 1928; Faure et al. 1973; Faure 1975; Hoang et al. 1974, 1996; Taviani et al. 1986; Dullo 1986, 1990; Plaziat et al. 1989, 1995, 1998, 2008; Hoang and Taviani 1991; Bosworth and Taviani 1996; El-Asmar 1997; El-Sorogy 1997; Taviani 1998a; Dawood et al. 2013; Bantan et al. 2015; Hamed 2015; Mansour and Madkour 2015; Hamed et al. 2016). An extensive flight of Pleistocene marine terraces equally borders both sides of the narrow and deep Gulf of

N. M. A. Rasul and I. C. F. Stewart (eds.), *Geological Setting, Palaeoenvironment and Archaeology of the Red Sea*,
https://doi.org/10.1007/978-3-319-99408-6_16

Aqaba, along the Sinai Peninsula and Jordan-Saudi Arabian coastline, and also occurs on Tiran Island (Hume 1906; Schick 1958; Goldberg and Yaron 1978; Gvirtzman et al. 1977, 1992; Gvirtzman and Buchbinder 1978; Al-Sayari et al. 1984; Dullo 1984, 1990; Al-Rifaiy and Cherif 1988; Strasser et al. 1992; Gvirtzman 1994; Bosworth and Taviani 1996; Strasser and Strohmenger 1997; Alhejoj et al. 2016; Manaa et al. 2016; Bosworth et al. 2017, and this volume). Furthermore, still-submerged Quaternary terraced reefs have been identified in the Gulf of Aqaba (Gvirtzman 1994; Hartman et al. 2015).

This type of coastal feature testifies to sea-level fluctuations during the Pleistocene (e.g., Aharon and Chappell 1986; Montaggioni and Braithwaite 2009; Lambeck et al. 2011; Camoin and Webster 2015; Dutton et al. 2015), but their current altitude with respect to the present mean sea level (m.s.l.) also responds to tectonic movements, a case often documented in the Red Sea (Faure 1975; Goldberg and Yaron 1978; Faure et al. 1980; Dullo 1990; Hoang and Taviani, 1991; Bosworth and Taviani 1996; El-Asmar 1997; Bosence et al. 1998; Bosworth et al. 2017, and this volume).

The raised Pleistocene coral terraces of the Red Sea region are known to pertain to various interglacial times, as supported by information based on dating techniques (e.g., Berry et al. 1966; Veeh and Giegengack 1970; Conforto et al. 1976; Goldberg and Yaron 1978; Andres and Radtke 1988; Dullo 1990; Gvirtzman et al. 1992; Choukri et al. 1995; Plaziat et al. 1998; Taviani 1998a; Dawood et al. 2013: but see Plaziat et al. 2008 warning about potential age errors and caveats linked to coral diagenesis). Most of them formed during the Marine Isotope Stage 5e (MIS5e) at about 125 ka BP (Dabbagh et al. 1984; Dullo 1990; Hoang and Taviani 1991; Gvirtzman et al. 1992; El-Moursi et al. 1994; Bosworth and Taviani 1996; Hoang et al. 1996; El-Asmar 1997; Plaziat et al. 1998, 2008; Walter et al. 2000; Scholz et al. 2004; Manaa et al. 2016; Bosworth et al. 2017; Casazza 2017; Al-Mikhlafi et al. 2018).

The Red Sea fossil coral reef systems host a remarkable paleobiological legacy which is useful to reconstruct former environments, to recognize past biodiversity, to unravel biogeographic connections and disclose paleoclimatic events (e.g., Newton 1900; Hall and Standen 1907; Cox 1929; Brighton 1931; Nardini 1937; Selli 1973; Dollfus and Roman 1981; Borri et al. 1982; Dullo 1990; Marchesan and Taviani 1994; Taviani 1994, 1998b; Ragani 1997; Plaziat et al. 1998; Mewis and Kiessling 2013; El-Sorogy et al. 2014; Bantan et al. 2015; Hamed 2015; Alexandroff et al. 2016; Angeletti et al., this volume). The marine terraces also provide pristine biogenic carbonates that are the prime material for dating purposes (Ivanovich and Harmon 1992) and are critical material for geochemically-based paleoclimate reconstructions (e.g., El-Asmar 1997; Felis et al. 2000, 2004; McCulloch and Esat 2000; Rimbu et al. 2001).

As reported above, MIS5e and older coral terraces have previously been studied and dated in the Gulf of Aqaba, but observations were not sufficient to provide a detailed assessment of Pleistocene vertical movements, nor were the coral terrace measurements combined with other types of structural data. Therefore, an expedition was conducted in winter 2013 to study the coastal terraces located on the Saudi Arabian part of the Gulf of Aqaba. This survey covered more than four fifths of the entire length of the Gulf's eastern coastal strip. One of the key objectives of this expedition was to obtain enough control points to determine where uplift is occurring along the Saudi Arabian margin of the Gulf of Aqaba, what the rate of that uplift (or subsidence) is, and what faulting style might be producing these vertical changes. The tectonic interpretation of the specific coral elevations calibrated by geological and radiometric data is discussed in Bosworth et al. (2017, and this volume), whilst preliminary results on the superb MIS5e fauna is reported by Angeletti et al. (this volume).

The goal of the present chapter is set at providing introductory information on the coastal terraces outcropping along the Saudi Arabian Gulf of Aqaba. These Pleistocene features surely deserve to be considered in the future for better stratigraphic assessment and accomplishing accurate facies reconstructions, inclusive of the pre-MIS5e carbonates, as well as for their paleoclimatic potential.

2 Materials and Methods

The winter 2013 expedition (December 6–15, 2013) was conducted by an international geological team under the leadership of the Saudi Geological Survey (SGS) in Jeddah, which supplied vehicles, full field work logistics and technical assistance (Bosworth et al. 2013). In particular, the SGS Lidar survey group has provided geomorphologic/topographic data for most stations that were surveyed. We explored the Saudi Arabian coastal strip of the Gulf of Aqaba from the border with the Kingdom of Jordan in the north to the Straits of Tiran in the south, a distance of about 140 km. Cursory observations were recorded at 27 principal stations along the coastline (Fig. 1, Table 1). In order to obtain a better appreciation of the Pleistocene reef systems, an exploratory SCUBA diving survey was also conducted for comparative purposes on a modern fringing reef 2.3 km south of Al Wasel (in front of St. 16).

Qualitative geo-paleontological sampling was conducted at most sites and the obtained material later shipped to ISMAR-CNR Bologna to be examined in the laboratory. Corals and other carbonate material (e.g., botryoidal aragonite) suitable for dating purposes by the U-series method were collected and elevations measured in most cases by Lidar survey. Uranium and thorium isotopes were analyzed

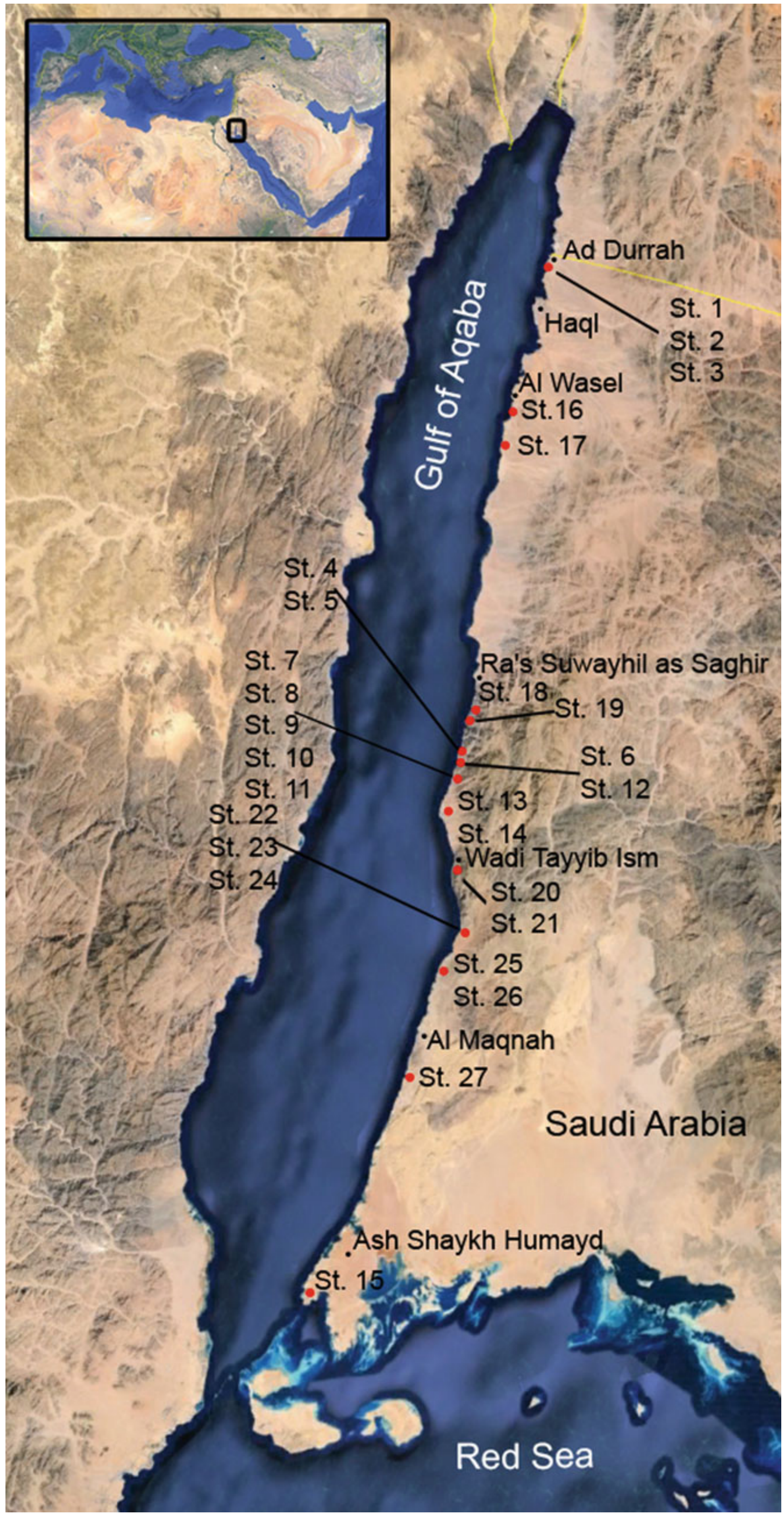

Fig. 1 Map of the Gulf of Aqaba showing the location of the stations discussed in the text (inset shows the regional geographic position of the Gulf of Aqaba)

Table 1 Station data of sites discussed in the text, indicating latitude and longitude, and terrace elevations above present m.s.l.; (*) marks elevation of terrace crests measured by Lidar. Note that station positions and altitudes correspond to those reported by Angeletti et al. (this volume); however, station numbers have been coded differently in Bosworth et al. (2017, and this volume), although from the same 2013 expedition

Station name	Latitude N	Longitude E	Elevation (m)
1*	29°21′19.60″	34°57′26.57″	11–13
2*	29°21′02.13″	34°57′23.09″	11
3*	29°20′19.18″	34°56′57.21″	14
4*	28°47′39.27″	34°49′33.02″	20
5*	28°46′46.89″	34°49′10.33″	19–23
6	28°45′29.59″	34°48′46.18″	23–25
7	28°42′36.15″	34°47′49.91″	22
8	28°42′30.28″	34°47′46.67″	22
9	28°42′24.91″	34°47′44.67″	22
10	28°42′26.44″	34°47′48.29″	22
11*	28°42′45.59″	34°47′52.91″	23
12*	28°46′06.37″	34°49′00.37″	25
13*	28°40′41.83″	34°46′52.21″	24
14*	28°40′32.74″	34°46′46.30″	19
15*	28°05′47.43″	34°34′21.16″	9
16*	29°11′22.95″	34°54′01.72″	19
17	29°11′09.33″	34°54′03.97″	19
18	28°48′36.63″	34°49′52.80″	19–26
19	28°48′32.05″	34°49′52.11″	19–27
20*	28°35′06.83″	34°47′35.14″	25
21	28°35′19.96″	34°47′32.39″	25
22*	28°30′23.94″	34°47′44.18″	18
23	28°30′17.31″	34°47′37.17″	14–22
24*	28°30′13.85″	34°47′39.01″	22
25*	28°26′58.80″	34°45′36.60″	26
26	28°26′23.32″	34°45′20.61″	26
27*	28°20′41.92″	34°43′09.55″	17

at the Laboratoire des Sciences du Climat et de l'Environnement (Gif-sur-Yvette, France) following laboratory procedures reported in Pons-Branchu et al. (2014). The U-series analysis was conducted only on pristine fossil material, identified based on a detailed mineralogical and petrographic screening of the entire coral collection. The U-series ages are presented in Bosworth et al. (2017) and are also reported in Table 2.

3 Geo-Structural Setting

The basement complexes of the Gulf of Aqaba region were accreted during the complex Neoproterozoic Pan-African orogenies that spanned from ~1000 to 540 Ma (Gass 1977; Kröner 1979; Stern 1994; Stern and Johnson 2010; Johnson and Kattan 2012). Granites and lesser metavolcanic rock

Table 2 U/Th dated MIS5e corals and botryoidal aragonite from the Saudi Arabian Gulf of Aqaba

Station name	Age (ka)	Note
6	125.56 ± 1.48	Fossil coral
8	118.58 ± 1.45	Botryoidal aragonite
15A	121.73 ± 0.96	Fossil coral
15D	120.14 ± 1.11	Fossil coral
16	121.54 ± 0.84	Fossil coral
22	122.76 ± 1.96	Fossil coral
24	117.42 ± 1.23	Fossil coral

types predominated in this area. The region was subsequently covered by a veneer of sedimentary rocks during the Paleozoic and Mesozoic, dominated by coarse siliciclastic continental deposits (Tawadros 2001; Guiraud et al. 2005). Much of this stratigraphic section was subsequently eroded, particularly during the Cenozoic Red Sea rifting event which initiated in this area at ~23 Ma (Coleman 1993; Bosworth et al. 2005). The Red Sea opened northward into modern day Egypt, stalling in the Neotethyan/Mediterranean margin (Steckler and ten Brink 1986). This finished creation of the Arabian plate, which at that time included Sinai. During the Middle Miocene, the Gulf of Aqaba—Dead Sea transform margin formed, and the Gulf of Suez was largely abandoned as an active continental rift (Bayer et al. 1988; Bosworth and McClay 2001). The Gulf of Aqaba evolved as series of pull-apart basins along this sinistral strike-slip plate boundary that now separates the Sinai micro-plate from the Arabian plate (Ben-Avraham et al. 1979; Bartov et al. 1980). The style of deformation within the basin is therefore dominated by strike-slip faulting which is attested to by the observed seismicity (Alamri et al. 1991; Roobol et al. 1999; Hofstetter 2003).

This strike-slip faulting will not, in and of itself, produce the significant uplift of the crystalline basement seen along its margins. This uplift could be formed at either extensional or convergent steps along the plate boundary, as in classical pull-apart basins or restraining bends. However, as noted by Ben-Avraham and Zoback (1992), the basin-margin (footwall) uplift is distributed along much of the Gulf of Aqaba rather than simply focused at the long-recognized intra-gulf left-stepping faults. The Gulf of Aqaba is experiencing a significant amount of opening perpendicular to its length, resulting in the descriptor of a "leaky" transform (Ben-Avraham et al. 1979). A large percentage of the small to moderate magnitude earthquakes in the Gulf are actually dip-slip normal fault events with ~ WNW-ESE tension axes (Alamri et al. 1991; Roobol et al. 1999; Hofstetter 2003). This component of extensional faulting along the length of the Gulf of Aqaba can be driving the uplift and exhumation of the basement complexes along the basin margins (Bosworth et al. 2017, and this volume).

In the study area, faulting was observed in both the strata and crystalline basement rocks beneath the coral terraces and within the carbonate units of the terraces themselves. Where kinematic data were present these faults are essentially all dip-slip and extensional in character; a few strike-slip faults of unknown age were observed in the basement granites (Bosworth et al., this volume).

In addition to general uplift of the Gulf of Aqaba margins the extensional faulting is also causing minor local tilting of the terrace units. We did not observe any significant horizontal repetition of terrace outcrops that could be attributed to extensional faulting.

4 The Coral Reef Terraces

Not surprisingly, when considering that a great percentage of the coastal area in the northern-central part of the narrow and deep Gulf of Aqaba (Figs. 1 and 2a) is rimmed by granitoid hills intruded by dikes of the Arabian basement complex reaching up to the present coastline, the modern coral reefs in the Gulf of Aqaba are narrow fringing reefs attached to the bedrock (Fig. 2b, c) with little if any development of back-reef lagoonal habitats (Mergner and Schuhmacher 1974; Bouchon et al. 1981; Gabrié and Montaggioni 1982; Dullo 1990; Dullo and Montaggioni 1998; Al-Horani et al. 2006). A few exceptions in the Saudi Arabian sector of the Gulf are offered by coasts facing wadi valleys and the lowlands to the south in the Midyan area (Fig. 2d, e). These accommodation space constraints hold valid also for their Pleistocene counterparts. This common physiography of limited beach development, absence of lagoons and extremely narrow fringing reefs is well exemplified at 2.3 km south of Al Wasel. This site has, therefore, been examined also for its modern reef facies, from shore to fore-reef, to complement the Pleistocene analysis and improve the facies interpretation (Figs. 3 and 4).

The coastal terraces rimming the Arabian side of the Gulf of Aqaba belong to more than one generation of reefal growth (Dullo 1984, 1990; Manaa 2011; Alhejoj et al. 2016; our own observations). Although the large majority of the terraces pertain to the last interglacial (MIS5e), older reefal limestone, possibly belonging to MIS7 (Manaa 2011) and older (Dullo 1990), occurs at many sites at places serving as substrate to the later development of MIS5e reefs. The degree of diagenesis, including more pronounced lithification and advanced dissolution of carbonate allochems (Dullo 1984, 1990), easily permits distinguishing older coral limestones from their last interglacial counterparts (Fig. 5). In the Red Sea region, most corals predating MIS5e reef growth suffered advanced to complete alteration and replacement of original aragonite into calcite, and the same holds true for aragonitic molluscs and cements alike (Gvirtzman and Friedman 1977; Dullo 1984, 1986). The difficulty of finding un-recrystallized corals in the pre-MIS5e is at present a major obstacle to establishing a sound chronological frame for all coral terraces in this region. We have concentrated on the better preserved and datable MIS5e systems.

The MIS5e coral reefs grew over older Pleistocene reefal limestones, Arabian basement crystalline rocks, and Miocene sedimentary rocks (Fig. 6). They attain present altitudes from about 5 m up to about 26 m above mean sea level (m.s.l.), thus indicating that this sector of the Saudi Arabian coastline underwent remarkable but also differential uplift since that time. Here we do not comment further on such neotectonic aspects which are instead fully discussed in Bosworth et al. (2017, and this volume). Because of the substantial uplift, 'deeper' parts of the former coral reef system, seldom exposed in outcrop, are visible.

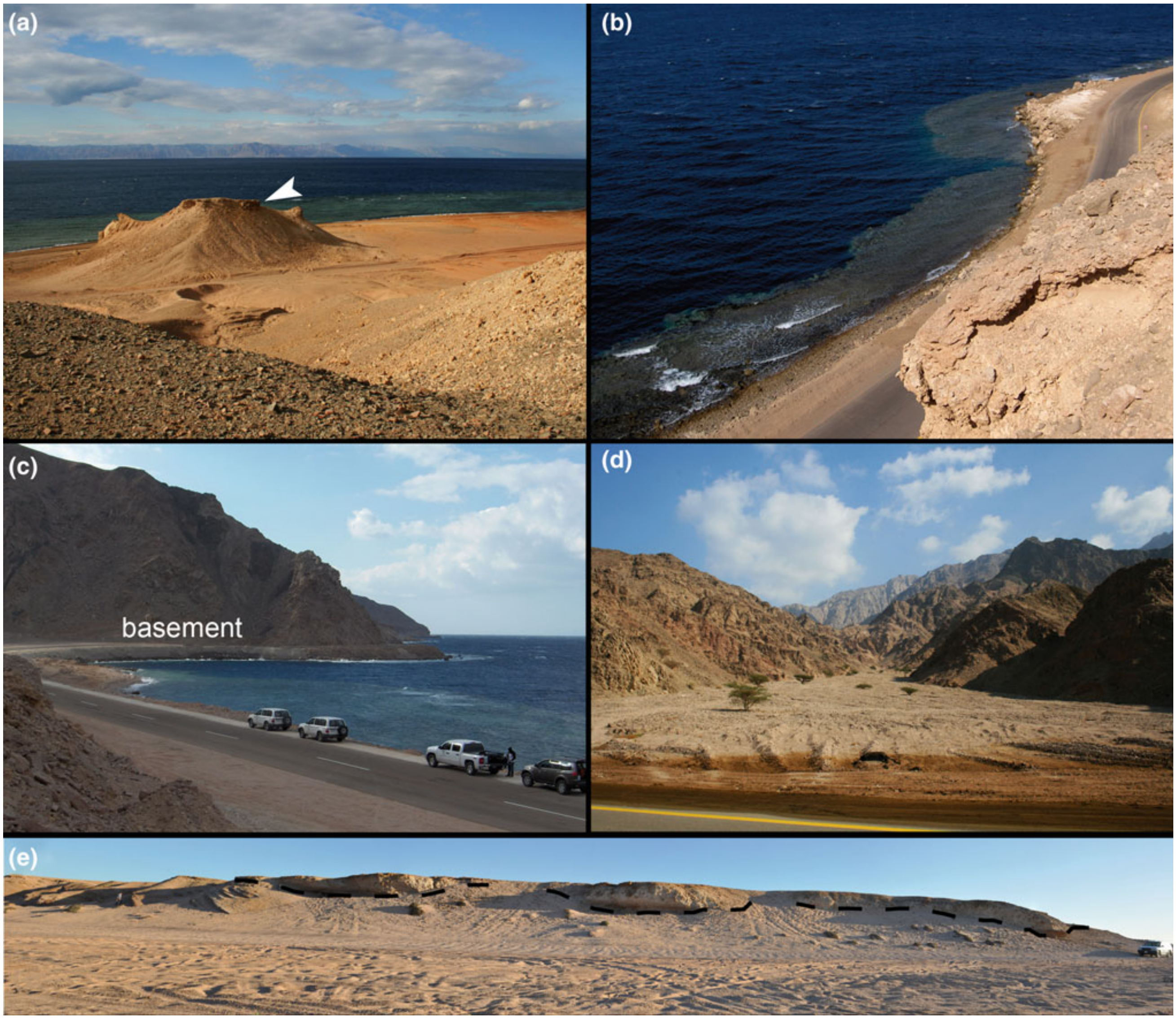

Fig. 2 Physiographic and geological constraints controlling coral reef development along the Saudi Arabian coast; **a** general view of the coast with alluvial plain, Pleistocene remnant of former reefs (arrow), modern sandy beach and fringing reef. Note in the background the mountain ranges of Sinai documenting the narrowness of the Gulf of Aqaba; **b** note the modest extension of the fringing reef hanging already at a few metres from the coastline in the deep waters of the Gulf of Aqaba, about 3 km north of Wadi Tayyib Ism; **c** the crystalline rocks of the Arabian basement reach up to the seashore along a considerable portion of the Saudi Arabian coast, about 4 km south of Ra's Suwayhil as Saghir; **d** lagoonal facies could in principle only develop on lowlands such as this wadi valley, prone to be invaded by the sea at times of relative high sea level, south of Ra's Suwayhil as Saghir; **e** general view of the southernmost tip of the Gulf, a lowland typified by Pleistocene reef growth in absence of uplifted bedrock, Ash Shaykh Humayd

5 Paleobiological Importance of the Pleistocene Coral Terraces

The Pleistocene terraces under scrutiny hold a remarkable fossil content of fundamental importance for reconstructing the former depositional and ecological environments and similarly for dating purposes. The pre-MIS5e carbonates have been by and large affected by diagenetic processes intense enough to dissolve in most cases any original aragonitic mineralogy. Calcitic fossils are often preserved (e.g., foraminifers, echinoids, pectinids). The MIS5e terraces are on the contrary little affected by diagenesis, leaving the aragonite record intact in many cases. This material is critical for identifying proper dating material, and, in perspective, may serve for paleoclimatic-oriented geochemical analyses.

The MIS5e macrofauna of these coral terraces is highly diverse and comprises scleractinian corals (*Acropora*,

Fig. 3 The modern fringing reef at Al Wasel explored by SCUBA diving on 11 December 2013: **a** general view of the site, the tabular relief on the right is St. 16; **b** tabular and shallow (50 cm) reef flat with predominant abraded, almost barren carbonate bedrock with algal coverage; **c** rippled sandy bottom with scant algal coverage and partly unburied carbonate substrate, 1 m depth (bar = 10 cm); **d** reef-edge and beginning of the reef slope showing intense coral growth, characterized by hydroids *Millepora platyphylla* (foreground) and *Millepora dichotoma* (isoriented fans), and scleractinians (*Porites* and *Acropora*, in the centre), about 1.5 m depth (bar = 10 cm); **e** reef slope, about 15 m depth, characterized by patchy coral colonies and sandy sediment; **f** outer reef at about 5 m, with scleractinian colonies (*Stylophora*, *Acropora*, faviids) and *Millepora* growing on dead coral limestone bedrock. Reef-edge and upper reef slope analog facies are represented in the visible part of the MIS5e terrace to the right. The MIS5e St. 16 includes back reef sandy habitats not occurring today at the diving spot. Underwater pictures by Abdulnasser Al-Qutub

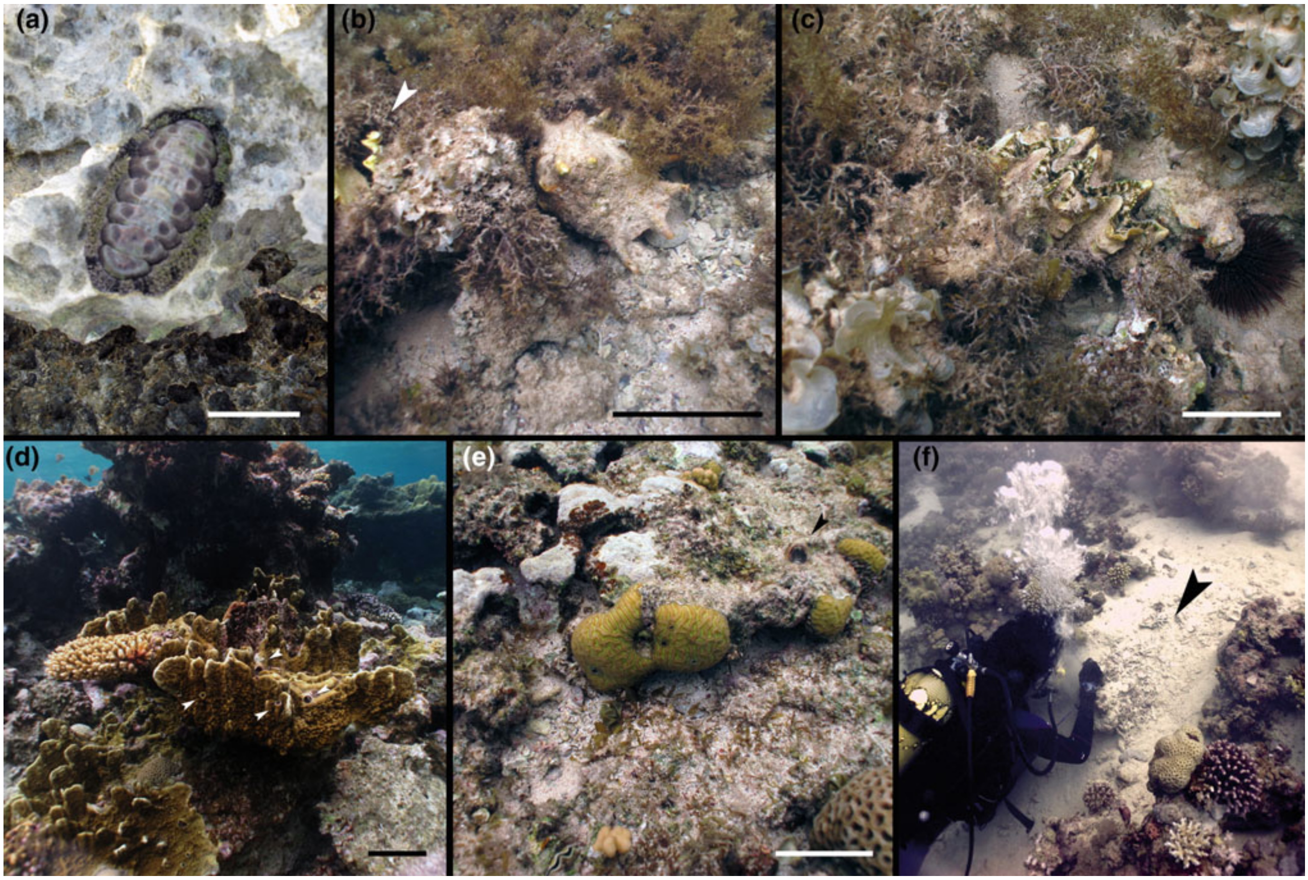

Fig. 4 Details of modern habitats at Al Wasel: **a** eroded reefal bedrock colonized by intertidal molluscs, such the chiton *Acanthopleura vaillantii* (bar = 1 cm); **b** the large gastropod *Lambis truncata sebae* camouflaged among algae on the reef flat; note dead but fresh *Tridacna* shell on the left (arrow) (bar = 10 cm); **c** gaping specimen of the large clam *Tridacna maxima* on the reef flat (bar = 10 cm); **d** reef edge at −1 m with eroded bedrock remnant and in the foreground a colony of *Millepora platyphylla* embedding various specimens of the giant vermetid gastropod *Ceraesignum maximum* (arrows) (bar = 5 cm); **e** reef edge with carbonate bedrock settled by scattered "faviid" corals and vermetids (arrow) (bar = 5 cm); **f** coarse sandy skeletal hash (arrow) along the reef slope, about −10 m. Underwater pictures by Abdulnasser Al-Qutub

Fungia, *Pocillopora*, *Stylophora*, *Porites*, *Pavona*, *Leptoseris*, *Lobophyllia*, *Caulastraea*, *Favites*, *Goniastrea*, *Platygyra*, *Cyphastrea*, *Echinopora*, *Dipsastraea*, *Phymastrea*, *Galaxea*, *Leptastrea*, etc.), octocorals, hydroids (*Millepora*), molluscs, decapods, barnacles, echinoids, serpulids, and calcareous algae. Scleractinian corals are the main framebuilders (work in progress), but molluscs are the most diverse group (>400 species; Angeletti et al. this volume). Additionally, a variety of benthic microfossils occur in these deposits, mainly foraminifera (*Quinqueloculina* and other miliolids, *Sorites*, *Peneroplis*, *Heterostegina*, *Amphisorus*, *Amphistegina*, *Acervulina*, etc.) and ostracods. Noticeably, epipelagic foraminifera (e.g., *Globigerinoides ruber*, *Orbulina universa*), thecosomatous pteropods (e.g., *Creseis clava*, *Limacina bulimoides*, *Heliconoides inflatus*), abundant species of the Gulf of Aqaba holoplankton (Reiss and Hottinger 1984), and calcified meroplankton are a significant component of the fossil assemblages identified in the MIS5e deposits (e.g., St. 8 and 12), documenting the relevance of a pelagic input which is amplified and facilitated by the reduced size of fringing reef systems directly hanging over the open sea.

The in-depth study of this rich Pleistocene fauna will hopefully contribute to various aspects of the biogeography of the Red Sea-Indian Ocean region and the evolution of their biota. It will hopefully impact the debate about the supposedly complete sterilization of the Red Sea biota in response to the establishment of highly-saline basinal conditions during the last glaciation (Reiss et al. 1980; Locke and Thunell 1988; Taviani 1998b). Such faunal annihilation was followed by a complete post-glacial renovation, including coral reefs (Gvirtzman et al. 1977; Taviani 1998c), but this hypothesis is somewhat challenged by genetic data on endemic fish (Dibattista et al. 2016). More generally, appreciation of any difference in the coral reef assemblages versus the modern counterparts also bears on the global

Fig. 5 Pre-MIS5e Pleistocene carbonates: **a** Panoramic view of St. 2, Ad Durrah exposing pre-MIS5e carbonates; **b** Spur consisting of pre-MIS5e carbonates, with modest pockets of MIS5e sediments, St. 3, Ad Durrah; **c** Limestone block showing the severity of carbonate dissolution in pre-MIS5e reefal rocks, St. 14, 17.9 km south of Ra's Suwayhil as Saghir; **d** degraded and recrystallized "faviid" coral head at St. 1, Ad Durrah

understanding of coral reef ecosystemic stability *versus* the paroxysmal ice ages of the Pleistocene (e.g., Taviani 1998c; Camoin and Webster 2015).

6 Site Description

Sites visited during the winter 2013 field trip are shown in Fig. 1 and relevant data are reported in Table 1. Here we briefly describe the main sites from the north (close to the border with the Kingdom of Jordan) to the southernmost site at the very end of the Gulf. A thorough study of these terraces was not possible during this exploratory survey but all sites presented here have been georeferenced and photographed to permit their easier identification in the field by other researchers. This very basic and preliminary information is intended to help in orienting further scientific research on such coastal features. The sites are described from north to south.

The first sites are three isolated outcrops, whose crests are between 10–14 m above m.s.l., found close to the Jordan border as distinct almost adjacent geomorphic expressions of Pleistocene coral carbonates; they occur as spurs in small coastal indentations at the locality of Ad Durrah.

Station 1: is a coastal spur made up by a composite carbonate body (Fig. 6a); the basal coral carbonate is of unknown Pleistocene age, and is plastered by younger but undated carbonates above; the carbonate bedrock hosts recrystallized coral heads (Fig. 5d) and is bored by *Lithophaga* mussels and settled by *Spondylus* bivalves; large coral heads occur on the upper part of the section; no MIS5e deposits have been clearly recognized here.

Station 2: is close to the south in the same small embayment and displays a rather similar geological situation (Fig. 5a); it exposes coastal marine sands enriched in pectinids and irregular echinoids (*Clypeaster* and *Laganum*) whose tests are aligned along the bedding.

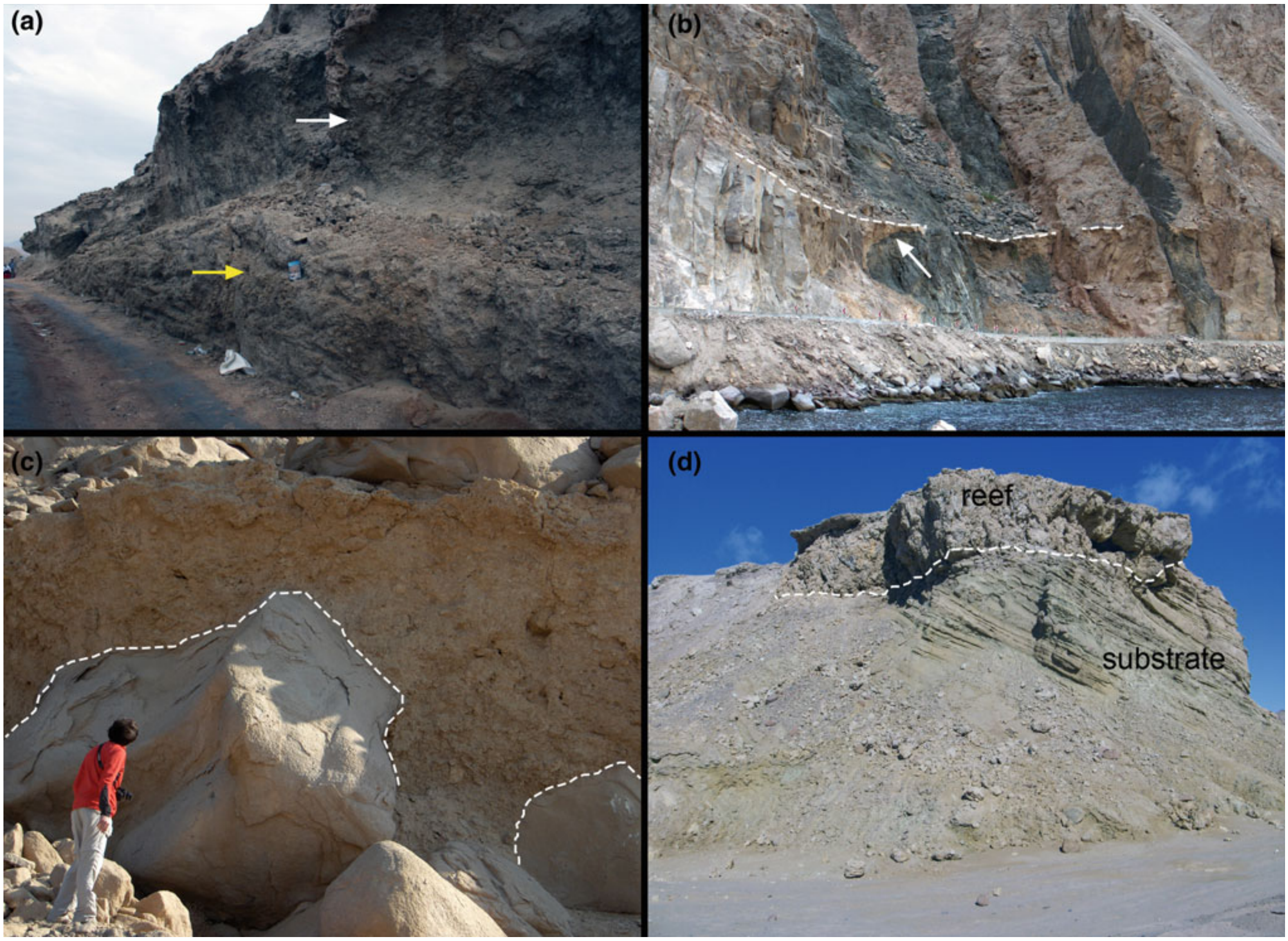

Fig. 6 Typology of contacts of MIS5e reefs with respect to substrate in the Saudi Arabian Gulf of Aqaba: **a** Young Pleistocene reef (white arrow) growing over preceding older Pleistocene reefs rocks (yellow arrow), St. 1, Ad Durrah; **b** remnants of MIS5e reefs (arrow) attached to Arabian basement rocks (granitoids crossed by basic dykes) at St. 12, 7.1 km south of Ra's Suwayhil as Saghir, dotted line marks the upper part of the reefal carbonates; **c** Reefal growth over large bedrock boulders (dotted line) at St. 6, 8.3 km south of Ra's Suwayhil as Saghir; **d** Reef growing over dipping Miocene sandstones (boundary between reefal carbonates and substrate marked by dotted line), St. 27, 6.75 km south of Al Maqnah

Station 3: is a small rocky spur immediately before the entrance fence of a coastguard site (Fig. 5b); besides older Pleistocene carbonates as at the previous two stations, last interglacial (MIS5e) reefal carbonates are exposed as documented by classic index-fossils, that is, the molluscs *Diodora impedimentum* and *Euplica turturina* (Taviani 1998a, 1998c).

Station 16: 2.3 km south of Al Wasel (Fig. 3a). This station is one of the best exposures of MIS5e coral terraces in the entire Gulf of Aqaba area coral reef systems, culminating at ~19–20 m above m.s.l. The preservation state of the host fossil content here is exquisite; noticeably fossiliferous, this site contains a *Pinna* bed with articulated shells amidst echinoids, other bivalves and gastropods. Corals are represented by a number of scleractinians (e.g., *Fungia*, *Acropora*, *Porites*, "faviids"), organ-pipe alcyonarians (*Tubipora*), and hydroids (*Millepora platyphylla*). The mollusc fauna of this terrace is one of the most diverse of the study area (Angeletti et al., this volume), representing various habitats including shore (the gastropods *Nerita orbignyana* and *N. sanguinolenta*), backreef (strombids, *Mammilla*, *Rhinoclavis*), reef-flat and edge (*Tectus dentatus, Trapezium oblongum*), and fore-reef (*Pinctada margaritifera*, *Spondylus* spp.).

Station 17: 2.65 km south of Al Wasel. The site exposes a poorly preserved reefal terrace, with degraded corals, *Tridacna* fragments, partly dissolved and replaced molluscs, including *Conus* spp., pectinids, and *Lithophaga* mostly as moulds; vestiges of ancient Pleistocene marine coral reef deposits are found at ~44 m above m.s.l.

Station 18: 2.4 km south of Ra's Suwayhil as Saghir. The site is represented by a granitic bedrock with carbonate veins and Neptunian dikes; some carbonate served as hardground substrate to encrusting serpulids.

Station 19: 2.45 km south of Ra's Suwayhil as Saghir. A spur-like outcrop of undated Pleistocene coral carbonates, macrofossiliferous, and at places cemented by botryoidal aragonite or bored by *Lithophaga*. Mixed carbonate-arkosic breccias (from the dismantling of the Arabian basement) also show cementation by aragonitic botryoids (Fig. 15c); the most recent reefal carbonates (MIS5e) contain molluscs and corals.

Station 4: 4.1 km south of Ra's Suwayhil as Saghir. MIS5e reefal terraces partly covered by alluvium along the coastal road at an elevation of ~20 m above m.s.l., are rich in well preserved frame-building scleractinian corals and molluscs; botryoidal aragonite cement occurs in the host rock (Fig. 15d).

Station 5: 5.8 km south of Ra's Suwayhil as Saghir. A fresh road cut exposes pre-MIS5e carbonate bedrock between 19–23 m above m.s.l.; next to the outcrop, loose but fresh *Porites* erratic blocks are found bored by *Lithophaga* mussels. This site was not examined in detail.

Station 12: 7.1 km south of Ra's Suwayhil as Saghir. Hanging Pleistocene coral limestones and semilithified carbonates plaster as relics the crystalline bedrock at 25 m above m.s.l. (Figs. 6b and 7d); this relic feature is extremely interesting since it documents a rare example of a late Pleistocene exposed slope, under pelagic input (pteropods, globigerinids) with-reef talus deposition. Abundant environmentally-valuable fossil material is found at this site, such as *Spondylus*, large barnacles and oysters on limestone bedrock, micromolluscs, melobesian fragments, decapod claws, rare corals, benthic foraminifers (including *Amphistegina*), ostracods, and echinoids in the loose or firm sediment.

Station 6: 8.3 km south of Ra's Suwayhil as Saghir. This outcrop is noticeable since it exposes large boulders overgrown by reefal carbonates attributable to MIS5e (Fig. 6c). This last interglacial fauna includes a variety of well-preserved scleractinian corals and molluscs, such as articulated (*Trapezium oblongum*) and disarticulated bivalves (*Spondylus* spp., *Trachycardium* sp.), and gastropods (e.g., Trochidae spp. and Cypraeidae spp.); large mamelon-like aragonite botryoids have been found here cementing Pleistocene reefal carbonates.

Station 7: 13.8 km south of Ra's Suwayhil as Saghir. A well-preserved flat-topped MIS5e coral terrace is exposed reaching up to ~22 m above m.s.l. (Fig. 7a–c). Fresh carbonates and scleractinian corals are exposed on the flanks along the wadi cut, revealing very large and articulated shells of the giant clam *Tridacna maxima*. The fossil system comprises a paleoshoreline, testified by *Cellana radiata* shells. The preservation of reef-building scleractinian corals is excellent, providing suitable material for geochronological dating and geochemical analyses.

Station 8: 14 km south of Ra's Suwayhil as Saghir. There is a large exposure of MIS5e reefal terraces at the same altitude as the previous station, with intervening bioturbated arkosic coarse-sandy deposits; the rich mollusc assemblage includes index-fossils such as *Diodora impedimentum* and *Euplica turturina*. This site is characterized by reef edge and upper slope abundant scleractinian corals including *Acropora*, *Porites*, *Caulastrea*, *Fungia* and "faviids" among others (Fig. 8d). The back-reef coarse coral sands host numerous articulated *Pinna* bivalves, and many other molluscs (especially common is *Architectonica trochlearis*). Finally, a MIS5e former shoreline is here documented by the limpet *Cellana radiata*.

Station 9: this site is immediately south of St. 8 and displays MIS5e tabular coral terrace remnants, some of which collapsed, and whose facies are equivalent to the previous station.

Station 10: this site is represented by a series of well-preserved coral terraces dissected by wadis at ~20 m above m.s.l. that is a conspicuous geomorphological aspect of the coastal plain at this location situated between stations 8 and 9 (Fig. 8a–c). Terraces consist of reefal facies enriched in scleractinian corals such as *Lobophyllia*, *Platygyra* (Fig. 8b), and molluscs as trochids, *Chicoreus ramosus, Spondylus* spp. and *Tridacna* sp. (Fig. 8c). This site is relevant for reconstructing the paleogeography and assessing post-depositional vertical movements since it keeps vestiges of the former last interglacial shoreline, also evidenced by outwashed worn shells of intertidal gastropods (*Cellana radiata*, *Nerita* sp.), other shallow marine molluscs (*Tridacna* sp., *Lambis truncata sebae*), and corals.

Station 13: 17.6 km south of Ra's Suwayhil as Saghir. The coral terraces reaching up to 25 m above m.s.l. (Figure 9a) display *Platygyra* colonies on top (Fig. 9b), and contain terebrid gastropods and sands with in situ *Tridacna* shells. The topmost coral rich carbonates cap a melobesian-rich whitish siliciclastic-carbonate sand, with scattered coral heads in situ (Fig. 9e). In this area we have identified a concentration of broken and bleached *Lambis* shells on the ground, possibly representing a sub-recent shell midden related to human activity (Fig. 9f).

Station 14: 17.9 km south of Ra's Suwayhil as Saghir. A complex coral reefal situation occurs at this site exposing un-dated Pleistocene coral bedrock affected by diagenetic processes, as documented by more or less completely dissolved corals and molluscs (Fig. 5c), and younger deposits with such features such as *Tridacna* beds, whitish melobesian sand, and frame-building corals.

Station 20: 3 km north of Wadi Tayyib Ism. This outcrop exposes the interfingering of MIS5e reefal carbonates with conglomeratic layers sitting on Arabian basement granitoids (Fig. 9c). Abundant scleractinian heads are observed in the

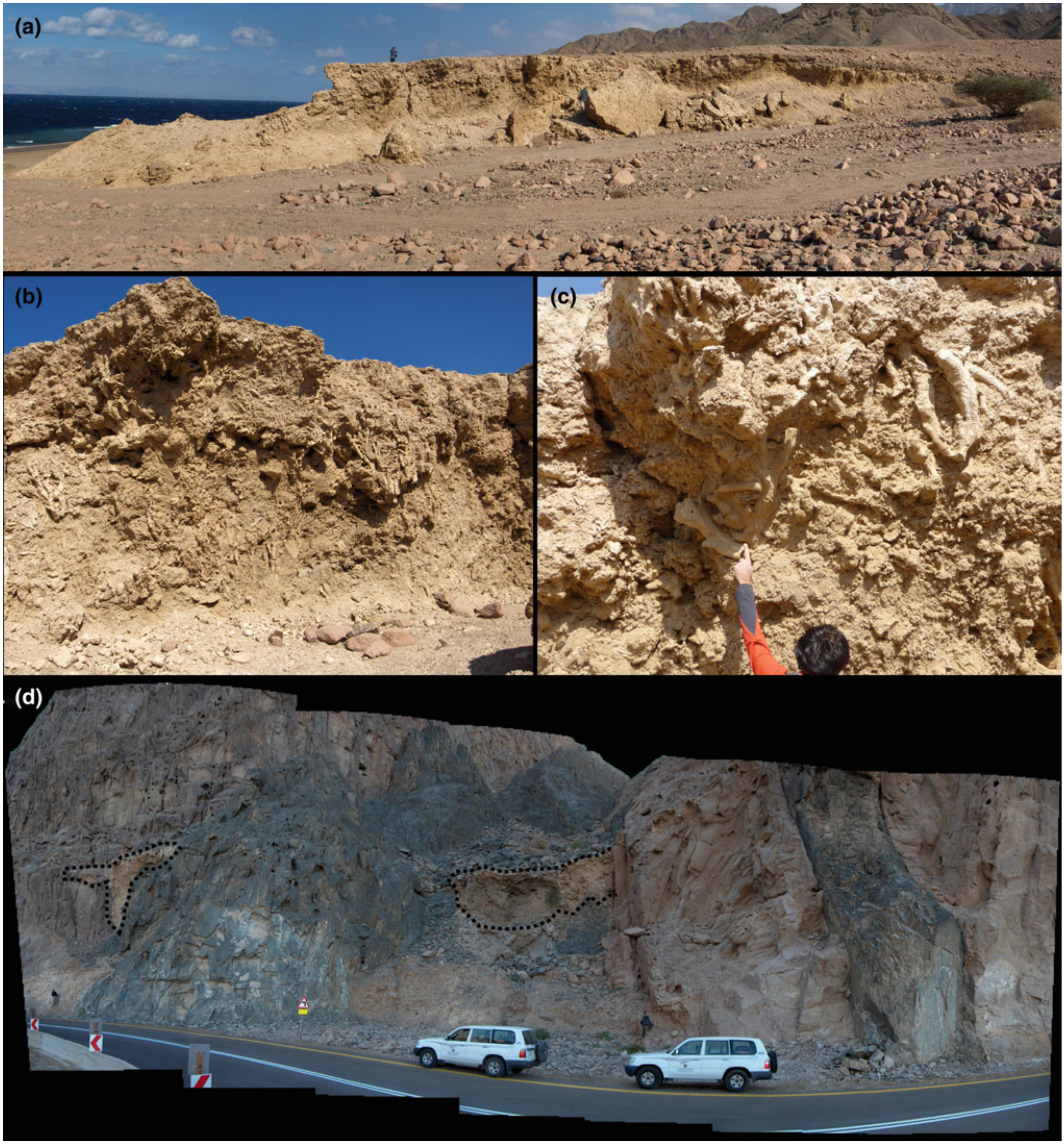

Fig. 7 **a** The MIS5e coral terrace 13.8 km south of Ra's Suwayhil as Saghir (St. 7); **b** an exposure of upper fore-reef coral-rich facies with numerous branching scleractinian corals; **c** detail showing large coral accumulation with *Porites*, "faviids" and other stony corals; **d** hanging Pleistocene coral limestones and semilithified carbonates plaster as relics (marked by dotted line) the crystalline bedrock, 7.1 km south of Ra's Suwayhil as Saghir (St. 12)

middle part of the section and are more common on the top carbonates, including *Porites*, *Acropora*, *Fungia* and "faviids". The accompanying benthic fauna includes the index-fossil *Diodora impedimentum*, and other gastropods (e.g., *Turbo radiatus, Ceraesignum maximum*), cemented (*Chama* spp., *Spondylus* spp.), epifaunal and infaunal bivalves (*Tridacna maxima, Trachycardium* sp.).

Station 21: 3.4 km north of Wadi Tayyib Ism, and before Al Maqnah. Here a presumed MIS5e coral growth at ~25

Fig. 8 **a** Well-preserved coral terraces at St. 10; **b** detail of an upper fore-reef facies typified by stony corals such as *Lobophyllia*, *Porites*, *Acropora* and "faviids"; **c** giant valve of *Tridacna maxima*; **d** underroof of a MIS5e tabular coral terrace remnants immediately to the south of St. 8 (St. 9) revealing various frame-building scleractinians such as *Galaxea*, *Lobophyllia*, *Porites* and *Acropora*

m above m.s.l. caps the Pliocene/Miocene bedrock; this outcrop has not been analyzed in detail.

Station 22: 5.9 km south of Wadi Tayyib Ism. This site consists of a cluster of three disconnected main outcrops culminating at altitudes between ~14–22 m above m.s.l., a few tens of metres apart separated by gullies on a wide coastal lowland. The reefal terraces (Fig. 10a–f) expose coral-rich facies, back-reef lagoonal red sands with marine

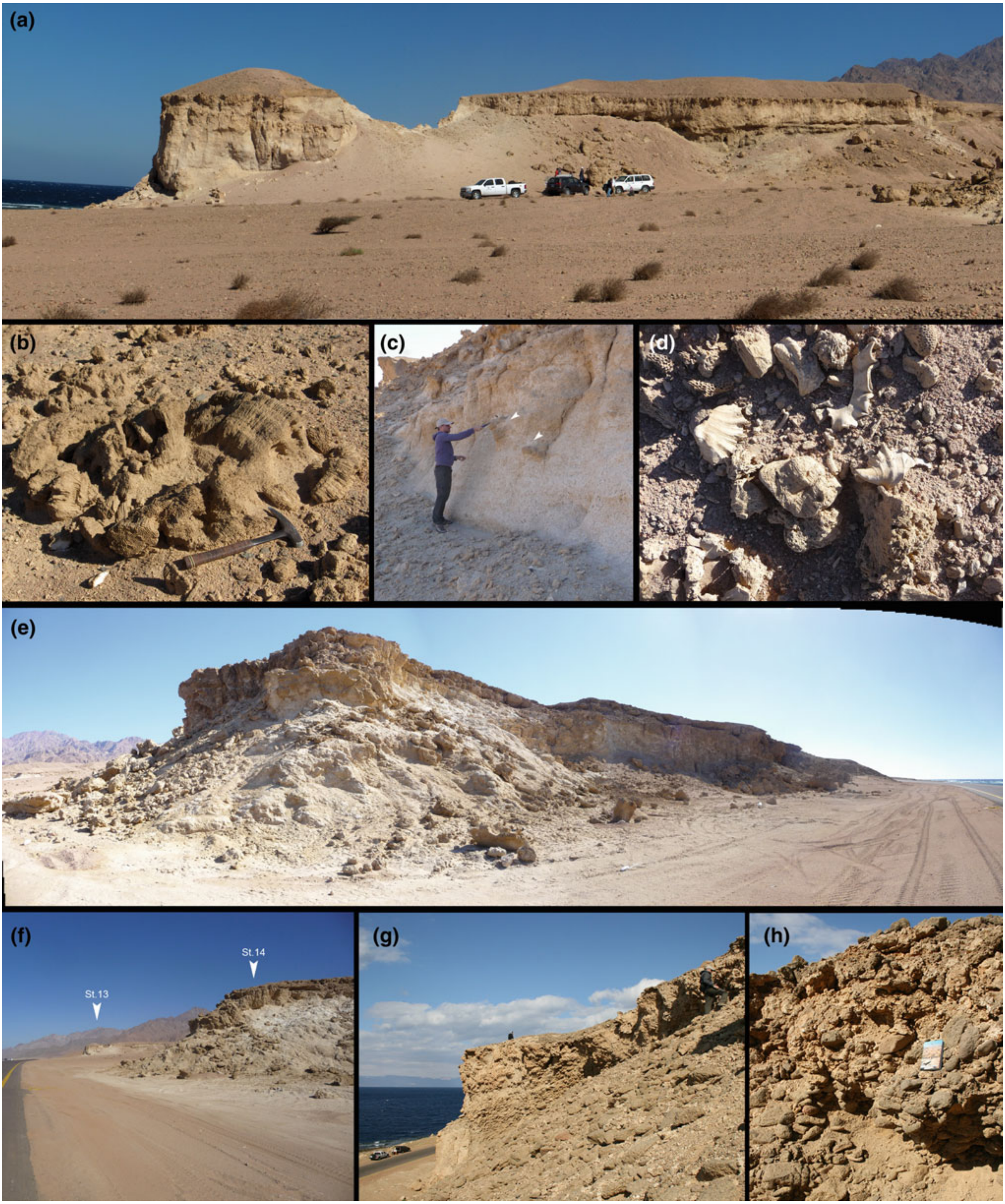

Fig. 9 **a** Coral terraces 17.6 km south of Ra's Suwayhil as Saghir (St. 13); **b** large *Platygyra* coral on the top of the terrace (St. 13); **c** small *Porites* coral heads (arrows) within siliciclastic-carbonate sand (St. 14); **d** broken *Lambis* shells scattered on the ground likely testify to a subrecent anthropogenic midden (St. 14); **e** coral terrace at St. 14; **f** general view of the sites showing relative positions of St. 13 and 14; **g** outcrop 3 km north of Wadi Tayyib Ism (St. 20) exposing the reefal carbonates, interfingering; **h** with basal conglomeratic deposits sitting on Arabian basement granitoids

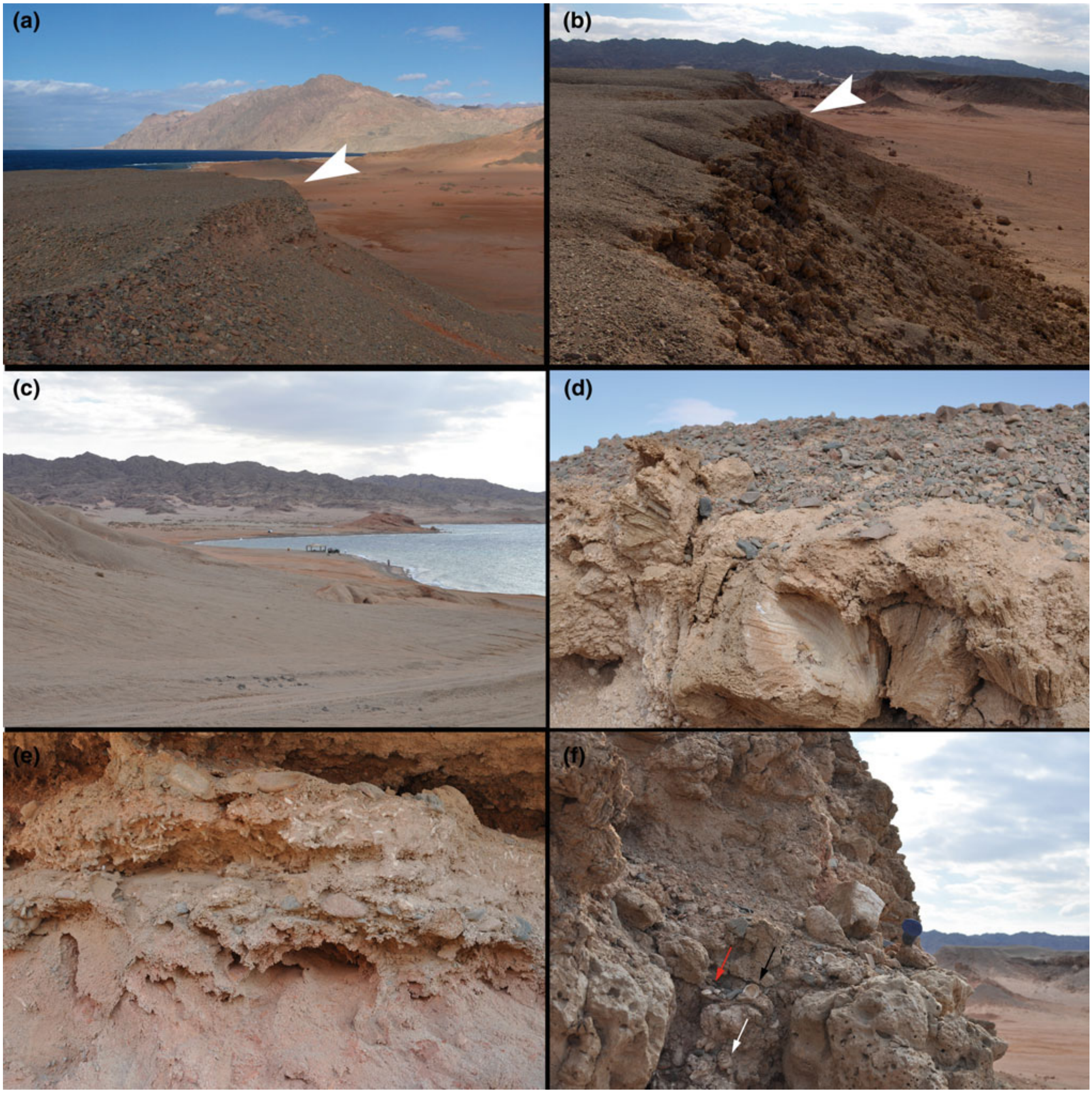

Fig. 10 **a**–**c** General views of the site 5.9 km south of Wadi Tayyib Ism (St. 22) consisting of three disconnected main MIS5e outcrops, a few tens of metres apart separated by gullies emerging on a wide coastal lowland, arrows pointing out the top of the terraces; **d** massive *Platygyra* heads on the top of the terrace; **e** intensely bioturbated (*Thalassinoides*) pebbly sand below reefal carbonates; **f** coarse reefal-sediment accumulation enriched by displaced skeletal remains, including echinoids (red arrow), bivalves (*Codakia tigerina*, black arrow) and gastropods (*Turbo radiatus*, white arrow)

molluscs (*Codakia tigerina*, *Lambis truncata sebae*), at places intensely bioturbated (*Thalassinoides*: Fig. 10e), and arkosic gravels. The raised reef deposit at ~12 m above m.s.l. hosts a dense coral growth mostly represented by well-preserved and large *Porites* heads (Fig. 10d), *Fungia*, "faviids", *Millepora* and other corals, which are draped by a veneer of coral debris which contains also highly degraded branching hydroids (*Millepora*) and molluscs.

Station 23: 6.1 km south of Wadi Tayyib Ism. The site is a MIS5e coral terrace whose dismantling sheds well preserved fossils in the talus.

Station 24: 6.2 km south of Wadi Tayyib Ism. The area is characterized by prominent coral terraces (Fig. 11a) and displays large coral heads on top but has not been analyzed in detail (Fig. 11b).

The Al Maqnah (or Maqna) area is described and commented in detail for its Pleistocene marine terraces by Dullo (1990).

Station 25: 5.6 km north of Al Maqnah. Here the faulted Miocene substrate is plastered by Pleistocene reefal deposits at 26 m above m.s.l. (Fig. 11c, d). The scant paleontological legacy includes clusters of the intertidal barnacle *Tetraclita*.

Station 26: 4.5 km north of Al Maqnah. This site exposes a flat-topped coral terrace flight at the same elevation as the previous station over Miocene sandstones (Fig. 12a), and is characterized by a rich coral content with *Lobophyllia*, *Acropora*, *Leptoseris*, *Platygyra*, *Stylophora*, *Porites*, *Fungia*, *Favites*, documenting a fore-reef setting (Fig. 12c, d); spectacular giant coral heads (*Galaxea fascicularis*: Fig. 12 b) are found here.

Station 27: 6.75 km south of Al Maqnah. A series of terraces around ~17 m above m.s.l. separated by gullies,

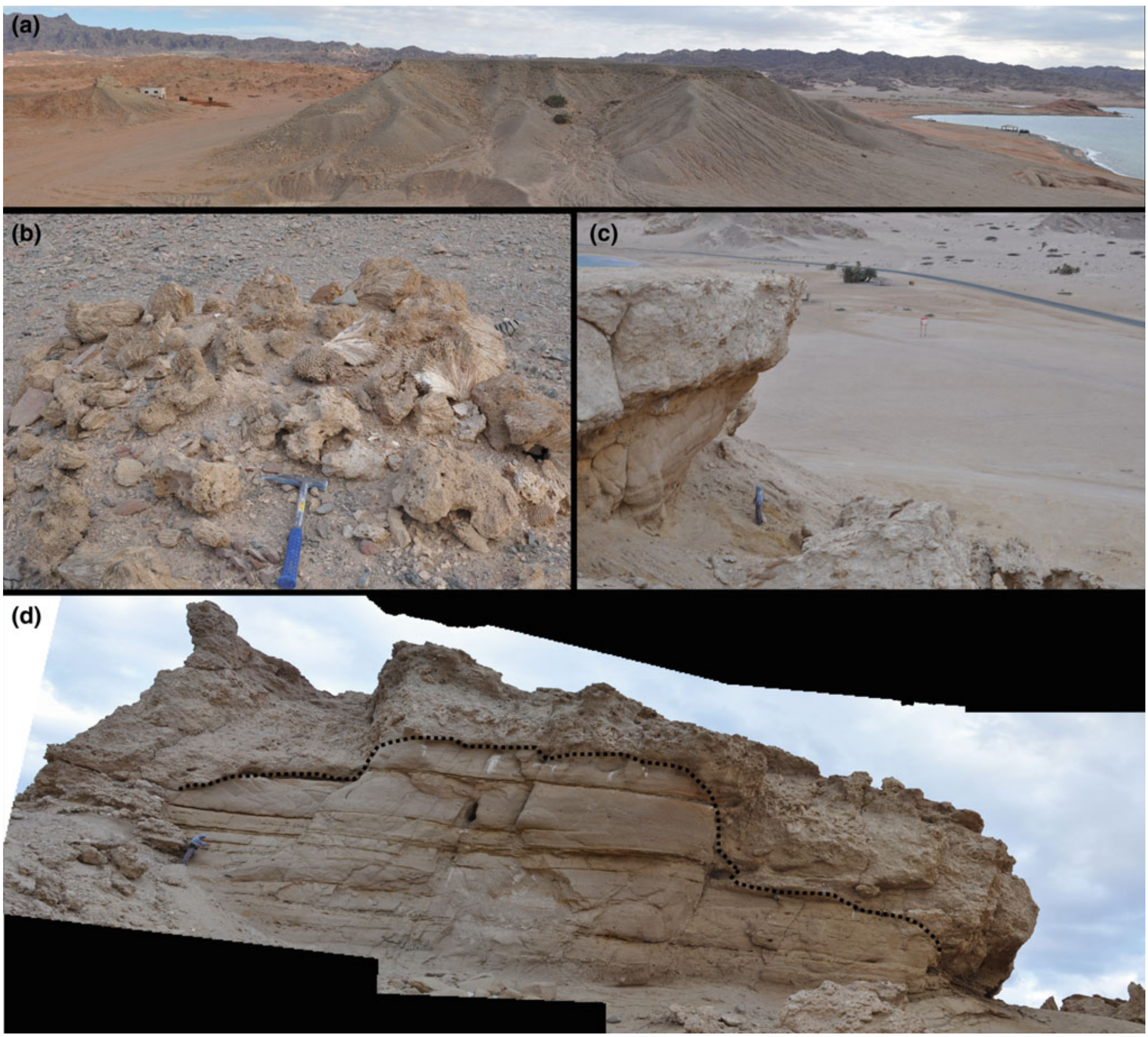

Fig. 11 **a** General view of the area 6.2 km south of Wadi Tayyib Ism (St. 24), characterized by prominent coral terraces; **b** detail of a coral terrace top showing large coral heads, prevalent *Platygyra* and "faviids"; **c**, **d** the faulted Miocene substrate 5.6 km north of Al Maqnah (St. 25), plastered by Pleistocene reefal deposits, dotted line marks the boundary between the MIS5e reef and the Miocene substrate, person for scale

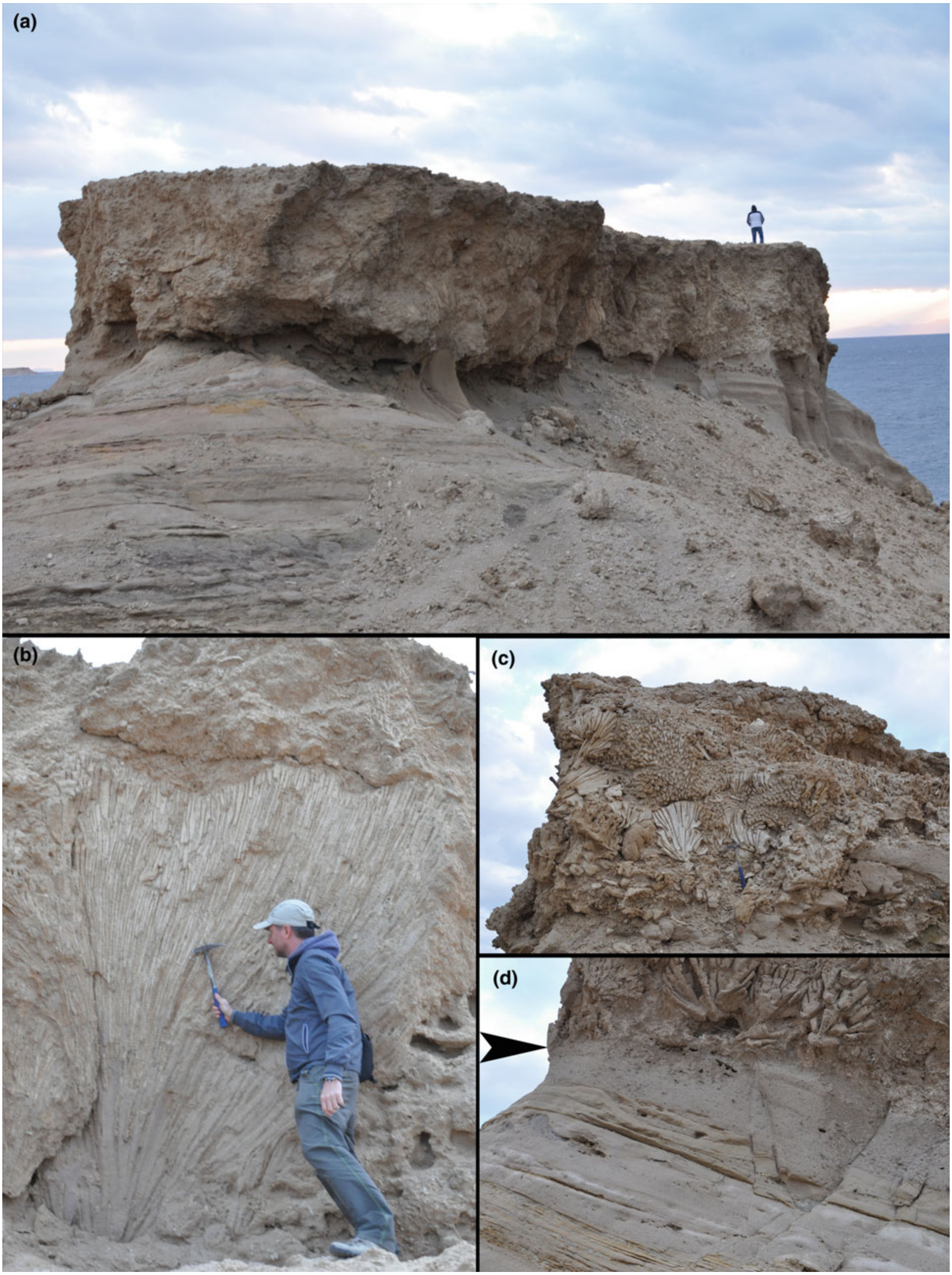

Fig. 12 **a** Flat-topped coral terrace capping Miocene sandstones, 4.5 km north of Al Maqnah (St. 26); **b** spectacular *Galaxea fascicularis* giant heads (>2 m in height) occur here; **c** outer-reef facies with *Lobophyllia hemprichii*, *Porites,* "faviids" and other stony corals; **d** detail of the contact between the MIS5e reef and Miocene sandstones showing large *Porites* colonies in growth-position

typifies the coastal setting with MIS5e coral terraces growing onto dipping Miocene strata (Fig. 6d). *Porites*-dominated reefs and intervening sandy sediments host abundant and diverse associated fauna which includes large bivalves (e.g., *Tridacna* spp, *Codakia tigerina*) and gastropods.

Station 15: Ash Shaykh Humayd. At the extreme south of the Gulf of Aqaba facing the Straits of Tiran and unconformably overlying Miocene sandstones (Fig. 13), there is a noticeable exposure of MIS5e coral reef terraces reaching a maximum elevation of ~8.7 m above m.s.l., which also host typical index fossils (*Diodora impedimentum*, *Euplica turturina*). The terraces expose reef-edge and back-reef lagoonal deposits, the latter culminating at ~4–6 m above m.s.l. This site is extremely rich in well preserved and diverse macrofossils (Fig. 13), including various stony corals (*Porites*, *Acropora*, *Montastraea*, *Favia*, *Favites*, *Fungia*, etc.), a number of molluscs (the bivalves *Tridacna* spp., Tellinidae spp., *Circe* spp., the gastropods *Conomurex fasciatus*, Cypraeidae spp., *Conus arenatus, Bulla ampulla*, and many others; Fig. 13f), echinoids (clypeasterids and *Heterocentrotus*), *Tetraclita* barnacles, melobesians, and much more. Botryoidal aragonite has been also found here.

7 Pleistocene Salina-Mangal Terrace

A unique situation for the Saudi Arabian Gulf of Aqaba to date is found 13.5 km south of Ra's Suwayhil as Saghir (St. 11) where a hyperhaline (evaporitic) and mangal complex crops out (Fig. 14). The sub-horizontal terrace reaches up to ~23 m above m.s.l. (Fig. 14a). Stratigraphically, the sequence exposes at its base a few metres of clayey-sandy lagoonal sediments containing the diagnostic mangrove-associated brackish gastropod *Terebralia palustris* (see Angeletti et al., this volume), numerous shells of the euryhaline gastropod *Pirenella conica*, articulated shallow-infaunal bivalves (*Gafrarium* sp., *Anodontia* sp.: Fig. 14b), and disarticulated intertidal bivalve shells (*Atactodea striata*). This basal lagoonal salina-mangal sequence is followed upward by a lenticular chaotic deposit (flash-flood?) and then by sediments documenting a confined saline microbasin (Fig. 14c). The evaporitic sequence consists of about 1 m of laminated gypsified evaporites, entrapping occasional gastropod marine shells (*Nerita* spp. and *Turbo radiatus*, possibly transported by hermit crabs), then by 40 cm of selenitic gypsum cumulates with macrocrystals up to 4 cm in size (Fig. 14d, e); this unit is affected upward by a second chaotic unit, and the sequence ends up with a second package of laminated evaporites (Fig. 14c).

Although the lack of corals in this site prevents precise U-series dating, we tentatively attribute this complex to MIS5e because of its altitude that is comparable to coral terraces, absence of evident diagenesis, and sub-horizontality. Analogous situations of this age are part of the coastal stratigraphy of the Red Sea proper, and have been treated in detail by Plaziat et al. (1998, 2008) and Orszag-Sperber et al. (2001).

8 Botryoidal Aragonite

Large aragonite fans and botryoids up to 8 cm in diameter have been discovered on terraces south of Ra's Suwayhil as Saghir (St. 4, 8 and 19), and at Ash Shaykh Humayd in the extreme south of the Gulf, as filling vugs into MIS5e and pre-MIS5e reefal carbonate bedrock, at places also cementing mixed carbonate-arkosic breccias (Fig. 15). Botryoidal aragonite is a distinct form of calcium carbonate micro- to macrofabric characterized by a radial-fibrous growth often achieving a mamelon-like final shape (Fig. 15b). Botryoids form in a variety of contrasting genetic scenarios; subaerial caves (Ostermann et al. 2007; Fairchild and Baker 2012), marine hydrocarbon seeps (e.g., Roberts et al. 1993; Savard et al. 1996; Taviani 2001; Feng et al. 2008; Taviani et al. 2016), or shallow-marine settings (Ginsburg and James 1976; Aissaoui 1985). Regarding the latter, spectacularly large aggregates of botryoidal aragonite are found as epigenetic marine cements filling vugs in Quaternary shallow-water carbonates, preferentially reefal host-rocks, from various tropical localities including New Caledonia, Bahamas, Belize and the Red Sea (Ginsburg and James 1976; Taviani and Rabbi 1984; Aissaoui 1985; Grammer et al. 1993; Dill et al. 1998). In the Red Sea basin, botryoidal aragonite has been reported from Pleistocene coral reef terraces along the Egyptian mainland and islands, and proved to represent synsedimentary marine cements based on field and stable isotope data (Taviani and Rabbi 1984; Aissaoui 1985; Taviani et al. 1987). The Zabargad Island's aragonite includes the largest known such crystals and mineralizes not only carbonate rocks but also fissures in basic intrusives and mixed breccias (Moon 1923; El-Shazly et al. 1974; Bonatti et al. 1983; Taviani et al. 1987). Botryoidal fabric is known in the geological record since the Paleozoic (Mazzullo and Cys 1978; Aissaoui 1985; Lake 2004; Brachert et al. 2007), more often as calcite or partially-dolomitized pseudomorphs of the original aragonite.

The aragonite botryoids from the Saudi Arabian fossil reefs are interpreted as synsedimentary fast-growing marine cements, similarly to their Gulf of Mexico analogues (Grammer et al. 1993), or Red Sea equivalents (Aissaoui 1985; Taviani et al. 1987). Regarding the time of their genesis, botryoidal aragonite from a MIS5e terrace south of Ra's Suwayhil as Saghir (St. 8) provided a U/Th age of about 119 ka (Bosworth et al. 2017; Table 2). This figure is consistent with a process of marine carbonate precipitation

Fig. 13 **a** The MIS5e terrace of Ash Shaykh Humayd here culminating at about +6 m above m.s.l.; **b** overview showing the same MIS5e reefal terraces, person for scale (arrow); **c** section documenting that the MIS5e overlies unconformably the inclined Miocene strata, more shelly at the base, and upward grading into a reef edge facies with *Platygyra*, *Porites*, *Acropora* and "faviids", more abundant on the top, as well as *Heterocentrotus* spines; **d** detail of a reef-edge facies with in-situ *Favites* and other stony coral colonies, and articulated *Tridacna* (arrow); **e** melobesian and stony coral-rich facies with colonial scleractinians such as "faviids" and the solitary *Fungia scutaria* (arrow), and *Heterocentrotus* spines; **f** detail of a chaotic shell-rich deposit sourced from back-reef sandy habitat; the highly diverse paleontological content is dominated by molluscs, including the lagoonal gastropods *Conus arenatus* (Co), *Bulla ampulla* (B) and the bivalve *Circe* sp. (Ci), and subordinately, "faviids" and irregular echinoids

Fig. 14 The lagoonal salina-mangal complex 13.5 km south of Ra's Suwayhil as Saghir (St. 11), **a** general view of the outcrop, with muddy-sandy lagoonal and mangal (mangrove derived) sediment at the base, followed upward by evaporitic deposits; asterisk marks the best stratigraphic exposure; **b** detail of the lagoonal salina-mangal sediments showing articulated *Anodontia* and *Gafrarium* bivalves still in situ (arrow); **c** the stratigraphy of the uppermost part of the evaporitic section (asterisk in a), documenting the top of the first laminite unit partly masked by talus (1), the selenitic cumulate unit (2), the second chaotic unit (3) and the second laminite unit (4); **d** detail of the selenitic gypsum cumulates, observe inverse grading; **e** hand sample of large selenitic gypsum crystals

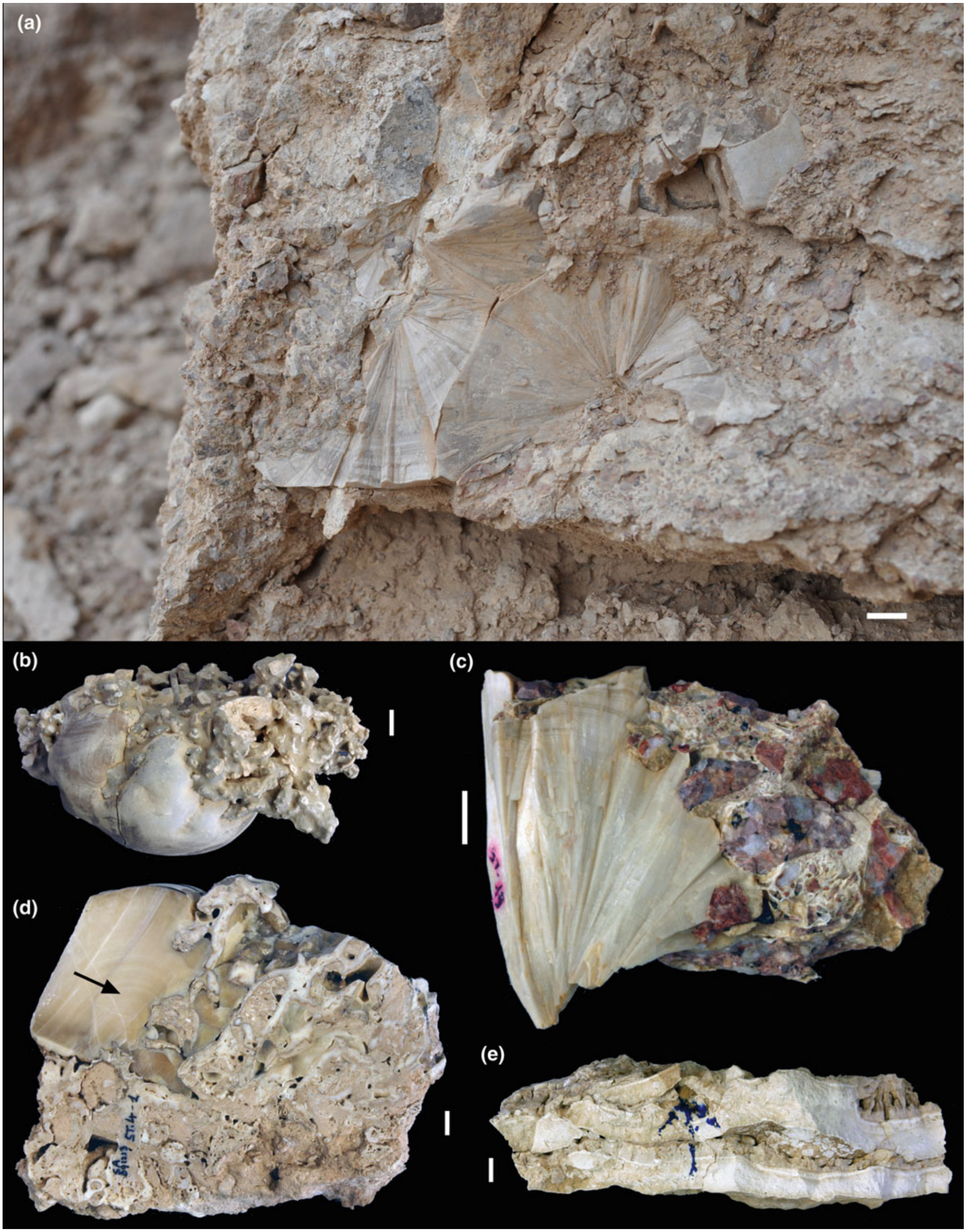

Fig. 15 Aragonite cements: **a** large fans within Pleistocene coral carbonates, 2.45 km south of Ra's Suwayhil as Saghir (St. 19); **b** mamelon-botryoid cementing Pleistocene reefal carbonates (St. 8); **c** mixed carbonate-arkosic breccia cemented by aragonite botryoids (St. 19); **d** polished slab of carbonate reefal bedrock showing large botryoidal aragonite cement, with clear accretionary bands (arrow) (St. 4); **e** drusy cements within vuggy carbonate rock (St. 19). Bars = 1 cm

during MIS5e, although this does not necessarily imply that all such aragonite cements observed in the terraces examined here share this age.

9 Summary and Conclusions

The Saudi Arabian coast of the Gulf of Aqaba boasts a superb set of marine coral terraces all along its length, connecting to the north with their equivalent in Jordanian territory and terminating to the south at the tip of the Arabian Peninsula and junction with the Red Sea. These terraces are Pleistocene in age, with the majority belonging to coral reef complexes of the last interglacial MIS5e. Besides coral reef terraces, this Pleistocene record also preserves a presumably coeval salina-mangal setting as well as spectacular examples of syndepositional aragonitic cement.

The altitude of the MIS5e terraces is variable, responding to tectonics, in most cases documenting considerable uplift. For future developments, it is important to note that the rich fossiliferous content provides a means to identify former environments with confidence, supplying ideal material for dating and geochemical paleoclimatology, and contributing taxonomic information valuable for evolutionary and biogeography purposes.

The exceptional uplift of MIS5e terraces makes these Saudi Arabian settings unique in the frame of the Red Sea region as a whole.

Acknowledgements We thank the Saudi Geological Survey for the invitation to present this study at the '2nd Red Sea Book Workshop' held in Jeddah on February 2016. The expedition in the Gulf of Aqaba has been promoted and funded by the Saudi Geological Survey in Jeddah. We acknowledge all participants to the Winter 2013 Field Party SGS personnel for field work (Ali Saeedi, Abdulnasser Al-Qutub, Salem Al-Nomani, Nawaf Widinly, Mostafa Khorshid, Thamer Bakarman) and post-expedition sample processing (Adel Jarees, Ali Al-Tharowi, Mohamed M. Bin Himd, Hassan Khamis Ali). Abdulnasser Al-Qutub was also part of the diving team and responsible for underwater photography. We thank Francesca Bosellini for helping with coral identification. Michele Morsilli and two anonymous referees provided valuable critical comments. This paper is part of PRIN2012 Programme (Project 20125JKANY_002, Principal Investigator Marco Ligi) and is Ismar-CNR, Bologna, scientific contribution no. 1905.

References

Aharon P, Chappell J (1986) Oxygen isotopes, sea-level changes and the temperature history of a coral reef environment in New Guinea over the last 105 years. Palaeogeogr Palaeocl 56:337–379

Aissaoui DM (1985) Botryoidal aragonite and its diagenesis. Sedimentology 32:345–361

Alamri AM, Schult FR, Bufe CG (1991) Seismicity and aeromagnetic features of the Gulf of Aqaba (Elat) region. J Geophys Res 96:20179–20185

Alexandroff SJ, Zuschin M, Kroh A (2016) Quantitative comparison of Pleistocene and Recent coral reef habitats in the northern Red Sea (El Quseir, Egypt). Facies 62:15. https://doi.org/10.1007/s10347-016-0468-6

Alhejoj I, Bandel K, Salameh E (2016) The fossil beach and reef terraces of the Gulf of Aqaba coast, Jordan—its environment, formation, and relation to mountain uplifting mechanism. Arab J Geosci 9:275. https://doi.org/10.1007/s12517-015-2293-6

Al-Horani FA, Al-Rousan SA, Al-Zibdeh M, Khalaf MA (2006) The status of coral reefs on the Jordanian coast of the Gulf of Aqaba, Red Sea. Zool Middle East 38:99–110

Al-Mikhlafi AS, Edwards LR, Cheng I (2018) Sea-level history and tectonic uplift during the last-interglacial period (LIG): Inferred from the Bab al-Mandab coral reef terraces, Southern Red Sea. J Afr Earth Sci 138:133–148

Al-Rifaiy IA, Cherif OH (1988) The fossil coral reefs of Al-Aqaba, Jordan. Facies 18:219–230

Al-Sayari SS, Dullo W-C, Hoetzl H, Jado AR, Zotl JG (1984) The Quaternary along the coast of the Gulf of Aqaba. In: Jado AR, Zotl JG (eds) Quaternary period in Saudi Arabia 2. Springer, Wien, pp 32–47

Andres W, Radtke U (1988) Quartäre strandterrassen an der küste des Gebel Zeit (Golf von Suez/Ägypten). Erdkunde 42:7–16

Angeletti L, Rasul N, Taviani M (this volume) Mollusc fauna associated with Late Pleistocene coral reef systems of the Saudi Arabian side of the Gulf of Aqaba

Bantan RA, Abu-Zied RH, Haredy RA (2015) Lithology, fauna and environmental conditions of the Late Pleistocene raised reefal limestone of the Jeddah coastal plain, Saudi Arabia. Arab J Geosci 8:9887–9904

Bartov Y, Steinitz G, Eyal M, Eyal Y (1980) Sinistral movement along the Gulf of Aqaba: Its age and relation to opening the Red Sea. Nature 285:220–221

Bayer H-J, Hötzl H, Jado AR, Roscher B, Voggenreiter W (1988) Sedimentary and structural evolution of the northwest Arabian Red Sea margin. Tectonophysics 153:137–151

Ben-Avraham Z, Zoback MD (1992) Transform-normal extension and asymmetric basins: An alternative to pull-apart models. Geology 20:423–426

Ben-Avraham Z, Garfunkel Z, Almagor G, Hall JK (1979) Continental breakup by a leaky transform: The Gulf of Elat (Aqaba). Science 206:214–216

Berry L, Whiteman AJ, Bell SV (1966) Some radiocarbon dates and their geomorphological significance, emerged reef complex of the Sudan. Z Geomorphol 10:119–143

Bonatti E, Clocchiatti R, Colantoni P, Gelmini R, Marinelli G, Ottonello G, Santacroce R, Taviani M, Abdel-Meguid AA, Assaf HS, El Tahir MA (1983) Zabargad (St. John's) Island: An uplifted fragment of sub-Red Sea lithosphere. J Geol Soc 140:677–690

Borri M, Sabelli B, Taviani M (1982) *Cypraea* (*Talparia*) *exusta* Sowerby, 1832, from the central Red Sea: New data. Lavori Soc Malacol Ital 103–107

Bosence DWJ, Al-Aawah MH, Davidson I, Rosen B, Vita-Finzi C, Whittaker L (1998) Salt domes and their control on basin margin sedimentation: a case study from Tihama Plain, Yemen. In: Purser BH, Bosence DWJ (eds) Sedimentation and tectonics of rift basins: Red Sea-Gulf of Aden. Chapman and Hall, London, pp 450–467

Bosworth W, McClay K (2001) Structural and stratigraphic evolution of the Gulf of Suez rift, Egypt: A synthesis. In: Ziegler PA, Cavazza W, Robertson AHF, Crasquin-Soleau S (eds) Peri-Tethys Mem 6: Peri-Tethyan Rift/Wrench Basins and Passive Margins. Mém Muséum Nat Hist Natur Paris 186, pp 567–606

Bosworth W, Taviani M (1996) Late Quaternary reorientation of stress field and extension direction in the southern Gulf of Suez, Egypt: Evidence from uplifted coral terraces, mesoscopic fault arrays, and borehole breakouts. Tectonics 15:791–802

Bosworth W, Huchon P, McClay K (2005) The Red Sea and Gulf of Aden Basins. In: Catuneanu O, Guiraud R, Eriksson P, Thomas B, Shone R, Key R (eds) Phanerozoic evolution of Africa. J Afr Earth Sci 43:334–378

Bosworth W, Taviani M, Rasul, N, Angeletti L, Montagna P, and Team (2013) Pleistocene Coral Terrace Project—Gulf of Aqaba, Saudi Arabia, Phase 1: December 6–15, 2013. SGS Report, 61 pp

Bosworth W, Montagna P, Pons-Branchu E, Rasul N, Taviani M (2017) Seismic hazards implications of uplifted Pleistocene coral terraces in the Gulf of Aqaba. Sci Repts 7(38):1–13. https://doi.org/10.1038/s41598-017-00074-2

Bosworth W, Rasul N, Taviani M (this volume) Neotectonics of the Red Sea, Gulf of Suez and Gulf of Aqaba

Bouchon C, Jaubert J, Montaggioni L, Pichon M (1981) Morphology and evolution of the coral reefs of the Jordan coast of the Gulf of Aqaba (Red Sea). Proc Fourth Intern Coral Reef Symp, Manila 1:559–565

Brachert TC, Vescogni A, Bosellini F, Reuter M, Mertz-Krauss M (2007) High salinity variability during the early Messinian revealed by stable isotope signatures from vermetid and *Halimeda* reefs of the Mediterranean region. Geol Romana 40:51–66

Brighton AG (1931) The geology of the Farasan Islands, Gizan and Kamaran Island, Red Sea. Part 3. Echinoidea. Geol Mag 68:323–333

Camoin G, Webster JM (2015) Coral reef response to Quaternary sea-level and environmental changes: State of the science. Sedimentology 62:401–428

Casazza LR (2017) Pleistocene reefs of the Egyptian Red Sea: Environmental change and community persistence. PeerJ 5:e3504. https://doi.org/10.7717/peerj.3504

Choukri A, Reyss JL, Plaziat JC (1995) Datations radiochimiques des hauts niveaux marins de la rive occidentale du Nord de la Mer Rouge au moyen de radioles d'oursins. CR Acad Sci Paris, (Sér 2, Sci Terre) 321:25–30

Coleman RG (1993) Geologic evolution of the Red Sea. Oxford Monographs on Geology and Geophysics, vol 24. Oxford University Press, Oxford, p 186

Conforto L, Delitala MC, Taddeucci (1976) Datazioni col 230Th di alcune formazioni coralligene delle Isola Dahlak (Mar Rosso). Rend Soc Ital Miner Petrol 32:153–158

Cox LR (1929) Notes on the post-Miocene Ostreidae and Pectinidae of the Red Sea region, with remarks on the geological significance of their distribution. Proc Malacol Soc London 18:165–209

Dabbagh A, Hoetzl H, Schnier H (1984) Farasan Islands. In: Jado AR, Zotl JG (eds) Quaternary period in Saudi Arabia 2. Springer, Wien, pp 212–220

Dawood YH, Aref MA, Mandurah MH, Hakami A, Gameil M (2013) Isotope geochemistry of the Miocene and Quaternary carbonate rocks in Rabigh area, Red Sea coast, Saudi Arabia. J Asian Earth Sci 77:151–162

Dibattista JD, Choat JH, Gaither MR, Hobbs J-PA, Lozano-Cortés DF, Myers RF, Paulay G, Rocha LA, Toonen RJ, Westneat MW, Berumen ML (2016) On the origin of endemic species in the Red Sea. J Biogeogr 43:13–30

Dill RF, Land LS, Mack LE, Schwarcz HP (1998) A submerged stalactite from Belize: Petrography, geochemistry, and geochronology of massive marine cementation. Carbon Evapor 13:189–197

Dollfus RP, Roman J (1981) Les echinides de la Mer Rouge. Monographie zoologique et paléontologique, Ministères des Universités, Comité des travaux historiques et scientifiques, Bibliothèque Nationale de Paris, 145 pp

Dreyfuss M (1931) Etudes de géologie et de géographie physique sur la cote francaise des Somalis. Rev Géogr Phys Géol Dyn 4:311–327

Dullo W-C (1984) Progressive diagenetic sequence of aragonite structures: Pleistocene coral reefs and their modern counterparts on the eastern Red Sea coast, Saudi Arabia. Palaeontogr Am 54:254–260

Dullo W-C (1986) Variation in diagenetic sequences: an example from Pleistocene coral reefs, Red Sea, Saudi Arabia. In: Schroeder JH, Purser BH (eds) Reef Diagenesis. Springer, Berlin, pp 77–90

Dullo W-C (1990) Facies, fossil record, and age of Pleistocene reefs from the Red Sea (Saudi Arabia). Facies 22:1–46

Dullo W-C, Montaggioni L (1998) Modern Red Sea coral reefs: a review of their morphologies and zonation. In: Purser BH, Bosence DWJ (eds) Sedimentation and tectonics of rift basins: Red Sea-Gulf of Aden. Chapman and Hall, London, pp 583–594

Dutton A, Carlson AE, Long AJ, Milne GA, Clark PU, DeConto R, Horton BP, Rahmstorf S, Raymo ME (2015) Sea level rise due to polar ice-sheet mass loss during past warm periods. Science 349 (6244). https://doi.org/10.1126/science.aaa4019

El-Asmar HM (1997) Quaternary isotope stratigraphy and paleoclimate of coral reef terraces, Gulf of Aqaba, South Sinai. Egypt. Quatern Sci Rev 16:911–924

El-Moursi M, Hoang CT, El Fayoumy IF, Hegab O, Faure H (1994) Pleistocene evolution of the Red Sea coastal plain, Egypt: Evidence from Uranium-series dating of emerged reef terraces. Quatern Sci Rev 13:345–359

El-Shazly EM, Saleeb GB, Zaki N (1974) Quaternary basalt in St. John's Island, Red Sea. Egypt. Egypt J Geol 18:137–148

El-Sorogy A (1997) Pleistocene coral reefs of southern Sinai, Egypt: Fossil record, facies analysis and diagenetic alterations. Middle East Research Center, Ain Shams University, Earth Sci Series 11:17–36

El-Sorogy A, Youssef M, Al-Sabrouty M, Al-Otaiby N (2014) Facies pattern and molluscan fauna of the Late Pleistocene raised coral reef of Rabigh area, Red Sea coast, Saudi Arabia. Indian J Geo-Mar Sci 43:1571–1580

Fairchild IJ, Baker A (2012) Speleothem science: from process to past environments. Wiley-Blackwell, 450 pp

Faure H (1975) Recent crustal movements along the Red Sea and Gulf of Aden coasts in Afar (Ethiopia and T.F.A.I.). Tectonophysics 29:479–486

Faure H, Hoang CT, Lalou C (1973) Structure et géochronologie (230Th/234U) des récifs coralliens soulevés à l'ouest du Golf d'Aden (T.F.A.I). Rev Géogr Phys Géol Dynam 15:393–403

Faure H, Hoang CT, Lalou C (1980) Datations 234U/230Th des calcaires coralliens et mouvements verticaux à Djibouti. Bull Soc Géol France 22:959–962

Felis T, Lohmann G, Kuhnert H, Lorenz SJ, Scholz D, Pätzold J, Al-Rousan SA, Al-Moghrabi SM (2004) Increased seasonality in Middle East temperatures during the last interglacial period. Nature 429:164–168

Felis T, Pätzold J, Loya Y, Moaz F, Nawar AH, Wefer G (2000) A coral oxygen isotope record from the northern Red Sea documenting NAO, ENSO, and North Pacific teleconnections on Middle East climate variability since the year 1750. Paleoceanography 15:679–694

Feng D, Cheng D, Roberts HH (2008) Sedimentary fabrics in the authigenic carbonates from Bush Hill: Implication for seabed fluid flow and its dynamic signature. Geofluids 8:301–310

Gabrié C, Montaggioni L (1982) Sedimentary facies from the modern coral reefs, Jordan Gulf of Aqaba, Red Sea. Coral Reefs 1:115–124

Gass IG (1977) The evolution of the Pan African crystalline basement in NE Africa and Arabia. J Geol Soc London 134:129–138

Ginsburg RN, James NP (1976) Submarine botryoidal aragonite in Holocene reef limestones, Belize. Geology 4:431–436

Goldberg M, Yaron F (1978) Th 230/U 234 ages of raised Pleistocene marine terraces on the Island of Tiran and the southeastern coast of Sinai with some tectonic implications. IAS 10th International Congress on Sedimentology. Jerusalem, Abs 1:258–259

Grammer GM, Ginsburg RN, Swart PK, McNeill DF, Jull AJT, Prezbindowski DR (1993) Rapid growth rates of syndepositional marine aragonite cements in steep marginal slope deposits, Bahamas and Belize. J Sedimen Petrol 63:983–989

Guiraud R, Bosworth W, Thierry J, Delplanque A (2005) Phanerozoic geological evolution of Northern and Central Africa: An overview. In: Catuneanu O, Guiraud R, Eriksson P, Thomas B, Shone R, Key R (eds) Phanerozoic evolution of Africa. J Afr Earth Sci 43:83–143

Gvirtzman G (1994) Fluctuations of sea-level during the past 400,000 years: The record of Sinai, Egypt (northern Red Sea). Coral Reefs 13:203–214

Gvirtzman G, Buchbinder B (1978) Recent and Pleistocene coral reefs and coastal sediments of the Gulf of Eilat. Tenth International Congress of Sedimentology, Jerusalem, Post-Congress Excursion Y4:163–191

Gvirtzman G, Buchbinder B, Sneh A, Nir Y, Friedman GM (1977) Morphology of the Red Sea fringing reefs: A result of the erosional pattern of the last-glacial-low-stand sea level and the following Holocene recolonization. 2e Symposium International sur les Coraux et Récifs Coralliens Fossils. Mem Bur Rech Min 89:480–491

Gvirtzman G, Friedman GM (1977) Sequence of progressive diagenesis in coral reefs. Am Assoc Petrol Geol Stud Geol 4:357–380

Gvirtzman G, Kronfeld J, Buchbinder B (1992) Dated coral reefs of southern Sinai (Red Sea) and their implication to the Late Quaternary sea-levels. Mar Geol 108:29–37

Hall WJ, Standen R (1907) On the Mollusca of a raised coral reef on the Red Sea coast. J Conch 12:65–68

Hamed B (2015) Pleistocene reefs of the Red Sea coast, Sudan: Depositional environments, fossil coral, age dating and diagenesis. Ph.D. Thesis, Technische Universität Berlin, 131 pp. https://doi.org/10.14279/depositonce-4414

Hamed B, Bussert R, Dominik W (2016) Stratigraphy and evolution of emerged Pleistocene reefs at the Red Sea coast of Sudan. J Afr Earth Sci 114:133–142

Hartman G, Niemi TN, Ben-Avraham Z, Tibor G, Al-Zoubi A, Sade RA, Hall JK, Akawi E, Abueladas A, Al-Ruzouq R, Makovsky Y (2015) Distinct relict fringing reefs in the northern shelf of the Gulf of Elat/Aqaba: Markers of Quaternary eustatic and climatic episodes. Sedimentology 62:516–540

Hoang CT, Dalongeville R, Sanlaville P (1996) Stratigraphy, tectonics and palaeoclimatic implications of uranium-series-dated coral reefs from the Sudanese coast of the Red Sea. Quatern Int 31:47–51

Hoang CT, Lalou C, Faure H (1974) Les récifs soulevés à l'ouest du golfe d'Aden (TFAI) et les hauts niveaux de coraux de la dépression de l'Afar (Ethiopie), géochronologie et paléoclimats interglaciaires. In: Les méthodes quantitatives d'étude des variations du climat au cours du Pléistocène. Colloq Internation Centre Nation Rech Scient, Paris, 219:103–114

Hoang CT, Taviani M (1991) Stratigraphic and tectonic implications of uranium-series-dated coral reefs from uplifted Red Sea Islands. Quatern Res 35:264–273

Hofstetter A (2003) Seismic observations of the 22/11/1995 Gulf of Aqaba earthquake sequence. Tectonophysics 369:21–36

Hume WF (1906) The topography and geology of the peninsula of Sinai (southern portion). Survey Dept Egypt, Cairo, p 280

Hume WF, Little WH (1928) Raised beaches and terraces of Egypt. First Rep Comm on Pliocene and Pleistocene Terraces, Paris, pp 9–15

Ivanovich M, Harmon RS (1992) Uranium-series Disequilibrium: Applications to Earth, Marine, and Environmental Sciences. Oxford University Press, Oxford, p 911

Johnson PR, Kattan FH (2012) The Geology of the Saudi Arabian Shield. Saudi Geological Survey, Jeddah, p 479

Kröner A (1979) Pan African plate tectonics and its repercussions on the crust of northeast Africa. Geol Rundsch 68:565–583

Lake JH (2004) Early marine cementation in Upper Devonian (Duperow Formation) carbonates in southwestern Saskatchewan. In: Summary of Investigations 2004, 1. Saskatchewan Geological Survey, Sask Industry Resources, Misc Rep 2004–4.1, CD-ROM, Paper A-6, 3 pp

Lambeck K, Purcell A, Flemming NC, Vita-Finzi C, Alsharekh AM, Bailey GN (2011) Sea level and shoreline reconstructions for the Red Sea: Isostatic and tectonic considerations and implications for homin migration out of Africa. Quatern Sci Rev 30:3542–3574

Locke S, Thunell RC (1988) Paleoceanographic record of the last glacial/interglacial cycle in the Red Sea and Gulf of Aden. Palaeogeogr Paleoclimatol Palaeocol 64:163–187

Manaa AA (2011) Late Pleistocene raised coral reefs in the eastern Red Sea—Rabigh, Saudi Arabia. M.Sc. Thesis, School of Earth and Environmental Sciences, University of Wollongong, Australia. http://ro.uow.edu.au/theses/

Manaa AA, Jones BG, McGregor HV, Zhao J, Price DM (2016) Dating Quaternary raised coral terraces along the Saudi Arabian Red Sea coast. Mar Geol 374:59–72

Mansour AM, Madkour HA (2015) Raised coral reefs and sediments in the coastal area of the Red Sea. In: Rasul NMA, Stewart ICF (eds) The Red Sea: the formation, morphology, oceanography and environment of a young ocean Basin. Springer Earth System Sciences, Berlin Heidelberg, pp 379–393

Marchesan M, Taviani M (1994) Biological modification of coral reef molluscan assemblages during a glacial-interglacial cycle (Red Sea, Egypt). Mem Descr Carta Geol It 52:57–58

Mazzullo SJ, Cys JM (1978) In-situ formation of botryoidal aragonite on Permian seafloor. Am Assoc Petrol Geol Bull 63:493

McCulloch MT, Esat T (2000) The coral record of last interglacial sea levels and sea surface temperatures. Chem Geol 169:107–129

Mergner H, Schuhmacher H (1974) Morphologie, okologie und zonierung von korallenriffen bei Aqaba (Gulf von Aqaba, Rotes Meer). Helgoländer Wissensc Meeresunt 26:238–258

Mewis H, Kiessling W (2013) Environmentally controlled succession in a late Pleistocene coral reef (Sinai, Egypt). Coral Reefs 32:49–58

Montaggioni LF, Braithwaite CJR (2009) Quaternary Coral Reef Systems, History, development processes and controlling factors. Developments in Marine Geology 5, Elsevier, 550 pp

Moon FW (1923) Preliminary geological report on St. John's Island (Red Sea). Geol Surv Egypt Government Press, Cairo, Egypt, p 36

Nardini S (1937) Molluschi delle spiagge emerse del Mar Rosso e dell'Oceano Indiano. Parte II (Lamellibranchi). Palaeontogr It 37:225–247

Newton RB (1900) Pleistocene shells from the raised beach deposits of the Red Sea. Geol Mag 7(500–514):544–560

Orszag-Sperber F, Plaziat F, Baltzer F, Purser BH (2001) Gypsum salina-coral reef relationships during the Last Interglacial (MIS 5e) on the Egyptian Red Sea coast: A Quaternary analogue for Neogene marginal evaporites? Sediment Geol 140:65–85

Ostermann M, Sanders D, Prager C, Kramers J (2007) Aragonite and calcite cementation in "boulder-controlled" meteoric environments on the Fern Pass rockslide (Austria): Implications for radiometric age dating of catastrophic mass movements. Facies 53:189–208

Plaziat J-C, Purser BH, Soliman M (1989) Localisaton et organisation interne de récifs coralliens immatures sur un cone alluvial du Quaternarie ancien de la Mer Rouge (Sud de l'Egypt). Géol Médit 16:41–59

Plaziat J-C, Baltzer F, Choukri A, Conchon O, Freytet P, Orszag-Sperber F, Purser BH, Raguideau A, Reyss J-L (1995)

Quaternary changes in the Egyptian shoreline of the northwestern Red Sea and Gulf of Suez. Quatern Int 29–30:11–22

Plaziat J-C, Baltzer F, Choukri A, Conchon O, Freytet P, Orszag-Sperber F, Raguideau A, Reyss JL (1998) Quaternary marine and continental sedimentation in the northern Red Sea and Gulf of Suez (Egyptian coast): Influences of rift tectonics, climatic changes and sea-level fluctuations. In: Purser BH, Bosence DWJ (eds) Sedimentation and tectonics of rift basins: Red Sea-Gulf of Aden. Chapman and Hall, London, pp 537–573

Plaziat J-C, Reyss J-L, Choukri A, Cazala C (2008) Diagenetic rejuvenation of raised coral reefs and precision of dating. The contribution of the Red Sea reefs to the question of reliability of the Uranium-series datings of middle to late Pleistocene key reef-terraces of the world. Carn Géol 4:1–40

Pons-Branchu E, Douville E, Roy-Barman M, Dumont E, Branchu P, Thil F, Frank N, Bordier L, Borst W (2014) A geochemical perspective on Parisian urban history based on U-Th dating, laminae counting and yttrium and REE concentrations of recent carbonates in underground aqueducts. Quatern Geochronol 24:44–53

Ragani L (1997) Echinoid fauna from the Quaternary fringing reef of Aqaba (Jordan). Palaeontogr It 84:1–19

Reiss Z, Hottinger L (1984) The Gulf of Aqaba: Ecological Micropaleontology. Ecological Studies 50, Springer Verlag, Berlin Heidelberg New York Tokyo, 355 pp

Reiss Z, Luz B, Almogi-Labin A, Halicz E, Winter A, Wolf M, Ross DA (1980) Late Quaternary paleoceanography of the Gulf of Aqaba (Eilat), Red Sea. Quatern Res 14:294–308

Rimbu N, Lohmann G, Felis T, Pätzold J (2001) Arctic Oscillation signature in a Red Sea coral. Geophys Res Lett 28(15):2959–2962

Roberts HH, Aharon P, Walsh MM (1993) Cold-seep carbonates of the Louisiana continental slope-to-basin floor. In: Rezak R, Lavoie DL (eds) Carbonate Microfabrics. Springer, Berlin, pp 95–104

Roobol MJ, Al-Rehaili M, Arab N, Celebi M, Halawani MA, Janjou D, Kazi A, Martin C, Sahl M, Showail A (1999) The Gulf of Aqaba Earthquake of 22 November, 1995: Its effects in Saudi Arabia. Saudi Arabian Deputy Ministry for Mineral Resources Technical Report BRGM-TR-99-16, 67 pp

Sandford KS, Arkell WJ (1928) Paleolithic Man and the Nile Valley in lower Egypt with some notes upon a part of the Red Sea littoral. A study of the regions during Pliocene and Pleistocene times. The University of Chicago Press, pp 1–189

Savard MM, Beauchamp B, Veizer J (1996) Significance of aragonite cements around Cretaceous marine methane seeps. J Sediment Res 66(3):430–438

Schick AP (1958) Tiran: The straits, the island, and its terraces. Israel Explor J 8(3):189–196

Scholz D, Mangini A, Felis T (2004) U-series dating of diagenetically altered fossil reef corals. Earth Planet Sci Lett 218:163–178

Selli R (1973) Molluschi quaternari di Massaua e di Gibuti. In: Missione Geologica A.G.I.P. nella Dancalia meridionale e sugli altopiani Hararini (1936–1938), Docum Paleont Accad Naz Lincei Roma 4:151-444

Steckler MS, ten Brink US (1986) Lithospheric strength variations as a control on new plate boundaries; examples from the northern Red Sea region. Earth Planet Sci Lett 79:12159–12173

Stern RJ (1994) Arc assembly and continental collision in the Neoproterozoic East African Orogen: implications for consolidation of Gondwanaland. Ann Rev Earth Planet Sci 22:319–351

Stern RJ, Johnson P (2010) Continental lithosphere of the Arabian Plate: a geologic, petrologic, and geophysical synthesis. Earth-Sci Rev 101:29–67

Strasser A, Strohmenger C (1997) Early diagenesis in Pleistocene coral reefs, southern Sinai, Egypt: Response to tectonics, sea-level and climate. Sedimentology 44:537–558

Strasser A, Strohmenger C, Davaud E, Bach A (1992) Sequential evolution and diagenesis of Pleistocene coral reefs (South Sinai; Egypt). Sediment Geol 78:59–79

Taviani M (1994) The ever changing climate: Late Quaternary paleoclimatic modifications of the Red Sea region as deduced from coastal and deep-sea geological data. In: Proc Egyptian-Italian Seminar on "Geosciences and Archeology in the Mediterranean Countries". Geol Survey of Egypt, Spec Publ 70:193–200

Taviani M (1998a) Post-Miocene reef faunas of the Red Sea: Glacio-eustatic controls. In: Purser BH, Bosence DWJ (eds) Sedimentation and tectonics of rift basins: Red Sea-Gulf of Aden. Chapman and Hall, London, pp 574–582

Taviani M (1998b) Axial sedimentation of the Red Sea Transitional Region (22–25 N): Pelagic, gravity flow and sapropel deposition during the late Quaternary. In: Purser BH, Bosence DWJ (eds) Sedimentation and tectonics of rift basins: Red Sea-Gulf of Aden. Chapman and Hall, London, pp 467–478

Taviani M (1998c) Stable tropics not so stable: Climatically driven extinctions of reef-associated molluscan assemblages (Red Sea and western Indian Ocean; last interglaciation to present). In: Camoin GF, Davis G (eds) Reefs and Carbonate platforms in the Pacific and Indian oceans. Spec Publ Intl Assoc Sedimentologists, pp 69–76

Taviani M (2001) Fluid venting and associated processes. In: Martini P (ed) Vai GB. The Apennines and adjacent Mediterranean Basin. Kluwer Academic Publishers, Anatomy of an Orogen, pp 351–366

Taviani M, Franchi F, Angeletti L, Correggiari A, Lopez Correa M, Maselli V, Mazzoli C, Peckmann J (2016) Biodetrital carbonates on the Adriatic continental shelf imprinted by oxidation of seeping hydrocarbons. Mar Petrol Geol 66:511–531

Taviani M, Hoang C-T, Pini A, Rabbi E (1987) Massive aragonite submarine lithification of reefal and non-reefal host rocks: Examples from the Red Sea. 8th IAS Regional Meeting of Sedimentology, Tunis (Tunisia), 1–3 April 1987, Abstracts, pp 534–535

Taviani M, Rabbi E (1984) Marine botryoidal aragonite in Pleistocene reef limestones of Red Sea offshore islands (Northern Brother and Rocky Island). Min Petrogr Acta 27:49–56

Taviani M, Bonatti E, Colantoni P, Rossi PL (1986) Tectonically uplifted crustal blocks in the northern Red Sea: Data from the Brothers islets. Mem Soc Geol Ital 27(1984):47–50

Tawadros E (2001) Geology of Egypt and Libya. AA Balkema, Rotterdam, p 468

Veeh HH, Giegengack R (1970) Uranium-series ages of corals from the Red Sea. Nature 226:155–156

Walter RC, Buffler RT, Bruggemann JH, Guillaume MMM, Berhe SM, Negassi B, Libsekal Y, Cheng H, Edwards RL, von Cosel R, Néeraudeau D, Gagnon M (2000) Early human occupation of the Red Sea coast of Eritrea during the last interglacial. Nature 405(6782):65